UNIVERSITY OF CINCINNATI

Date: 10-Nov-2010

I, Raymond F Martell **,**

hereby submit this original work as part of the requirements for the degree of:

Master of Science

in Mechanical Engineering

It is entitled:

Investigation of Operational Modal Analysis Damping Estimates

Student Signature: Raymond F Martell

This work and its defense approved by:

Committee Chair: Randall Allemang, PhD
Randall Allemang, PhD

David Brown, PhD
David Brown, PhD

Allyn Phillips, PhD
Allyn Phillips, PhD

Investigation of Operational Modal Analysis Damping Estimates

A thesis submitted to the
Division of Research and Advanced Studies
of the University of Cincinnati

in partial fulfillment of the
requirements for the Degree of

MASTER OF SCIENCE

from the School of Dynamic Systems
of the College of Engineering and Applied Sciences

2010

By
Raymond F. Martell
B.S.M.E. University of Cincinnati, 2003

Abstract

Operational Modal Analysis has received a great deal of recent research and industry interest. This method has gained popularity due to potential for reduced test time and cost as well as application to large-scale structures where traditional modal analysis is difficult or impossible. Operational modal analysis has been shown to provide natural frequency and mode shape estimates that are equivalent to those delivered through traditional modal analysis. However, the damping estimates from the technique are often inaccurate.

This investigation focuses on the damping estimates delivered by traditional modal parameter estimation techniques when using output only data. Theoretical cases involving 5 degree-of-freedom and 15 degree-of-freedom systems are examined. Investigations into the effect of system damping and rank deficiency are also examined.

Acknowledgements

The road to finally finishing my thesis has been much longer and more difficult than I originally envisioned. The two most instrumental people involved are Dave Brown and Randy Allemang. They cannot be thanked enough for their help, guidance, understanding, and teaching ability. Dave's advice to never stop learning influenced me more than any other, possibly to a fault. The knowledge gained by following him on the road and through many conversations in the lab is truly invaluable. Randy's advice "Don't leave the lab until you're done" couldn't ring more true, and I wish I had only gotten to stick around a little longer until I was truly ready to go. I also can't thank him enough for getting me back on track when needed and providing valuable consultation and editorial help.

My wife Erin was the biggest help outside the lab. She took most of the downside of all the nights and weekends spent finishing this paper. She more than accommodated my love of learning and loathing of writing. Also to be commended are Todd Dahling and Matt Witter for the constant pokes and prods about getting done.

I also cannot forget all of the others in the lab whose company I enjoyed so much. Allyn Phillips, Dan Lazor and Shashank Chauhan who provided much help in the lead up work to this paper were invaluable to its completion. Also all the others who I was involved with in other studies (Jim, Mike, Dan, Sergey, Andy, and Justin), your camaraderie was much appreciated.

Table of Contents

Table of Figures

Tables

1 Introduction

The field of Operational Modal Analysis (OMA) has received a great deal of recent interest. Operational modal analysis is one of many terms for the process of extracting modal parameters from output or response only data. Traditional Experimental Modal Analysis (EMA) requires the measurement of the response of the system to a measured input force. The ability to estimate the modal parameters on structures where it is either difficult or impossible to measure the input forces to the system is very attractive. Thus, the technique lends itself well to bridges, wind turbines, oil platforms and other civil structures. This technique also has the potential to reduce test time and cost, two important factors for today's increasingly pressured design cycle times and budgets. Other factors in the increasing popularity of this method are the development of a number of new methods for analyzing this data, the availability of software products which deal specifically with OMA, and the addition of OMA capabilities in existing software.

Many aspects of OMA are similar or analogous to those of EMA. However, there are a number of intricacies that must be handled correctly to achieve acceptable results. Because OMA is closely tied with EMA, the background formulation of the Unified Matrix Polynomial Approach (UMPA) that was introduced by Allemang, Brown, and Fladung [1], can be applied.

The literature has shown that the natural frequencies and mode shapes estimated by OMA are accurate when compared to theoretical data or to results of EMA when used with test data. However, the damping estimates provided in these situations have been inaccurate or have not been investigated in-depth.

Chapter Two of this thesis provides a review of the background theory and illustrates the relationship of OMA to EMA A 5 degree-of-freedom analytical system is used to investigate

using traditional EMA methods with output-only data in Chapter Three. Chapter Three also studies the effect of the level of damping in the system on the damping estimates themselves. The effect of a lack of information (rank deficiency) on the damping is also investigated in Chapter Three. Chapter Four extends the investigations of EMA methods on output-only data and rank deficiency to a 15 degree-of-freedom system. Chapter Five then investigates some differences between frequency response functions and various power spectra.

2 Theoretical Background

The equations of motion of a discrete linear system can be expressed as a set of second order linear differential equations with *x* (response) and *f* (force) as a function of time:

$$[M]\{\ddot{x}(t)\}+[C]\{\dot{x}(t)\}+[K]\{x(t)\}=\{f(t)\} \quad \textbf{(1)}$$

Where *M, C, K* are the mass, damping, and stiffness matrices.

This can be transformed to the frequency domain with the form:

$$-[M]\{X(\omega)\}\omega^2+[C]\{X(\omega)\}j\omega+[K]\{X(\omega)\}=\{F(\omega)\} \quad \textbf{(2)}$$

Through algebraic manipulation the system characteristics (M, C, K matrices) which form the Frequency Response Function (FRF) matrix, the forcing function and the response vectors can be isolated in the form:

$$\left[-[M]\omega^2+[C]j\omega+[K]\right]\{X(\omega)\}=\{F(\omega)\} \quad \textbf{(3)}$$

The FRF is then easily identified in the following form:

$$[H(\omega)]=\left[-[M]\omega^2+[C]j\omega+[K]\right]^{-1} \quad \textbf{(4)}$$

The system response can then be written as the product of the FRF and the forcing function in the frequency domain.

$$\{X(\omega)\}_{N_o x1}=[H(\omega)]_{N_o x N_i}\{F(\omega)\}_{N_i x1} \quad \textbf{(5)}$$

There is currently no method to directly measure the mass, damping, and stiffness matrices experimentally. However, the response and forcing vectors can be experimentally measured.

These can be used to calculate cross-spectra and auto-spectra. From these spectra the FRF matrix can be estimated. There are a number of formulations for the calculation of the FRF matrix from these spectra, and the H_1 formulation follows as:

$$G_{XF}(\omega) = \{X(\omega)\}\{F(\omega)\}^H \tag{6}$$

$$G_{FF}(\omega) = \{F(\omega)\}\{F(\omega)\}^H \tag{7}$$

$$H_1(\omega) = \frac{G_{XF}(\omega)}{G_{FF}(\omega)} \tag{8}$$

The FRF matrix can also be expressed in terms of modal parameters in the following form.

$$[H(\omega)]_{N_o \times N_i} = [\Phi]_{N_o \times 2N_m} [j\omega[I] - [\Lambda]]^{-1}_{2N_m \times 2N_m} [L]_{2N_m \times N_i} \tag{9}$$

Where Φ is the modal vector matrix, Λ is a diagonal matrix containing the system poles, and L is the modal participation matrix which contains the modal scaling factor.

$$[L]_{2N_m \times N_i} = [Q]_{2N_m x 2N_m} [\Psi]_{2N_m xN} \tag{10}$$

Another way to state the relationship between the system characteristics, system response, and forcing function is a manipulation of Equation 4 with the form:

$$\{X(\omega)\}^H = \{F(\omega)\}^H [H(\omega)]^H \tag{11}$$

This can then be pre-multiplied by the response vector $\{X(\omega)\}$.

$$\{X(\omega)\}\{X(\omega)\}^H = \{X(\omega)\}\{F(\omega)\}^H [H(\omega)]^H \tag{12}$$

This can then be expanded to the following.

$$\{X(\omega)\}\{X(\omega)\}^H = [H(\omega)]\{F(\omega)\}\{F(\omega)\}^H [H(\omega)]^H \tag{13}$$

Then substituting the above equations is similar to the results from Bendat & Piersol below [1].

$$[G_{XX}(\omega)] = [H(\omega)][G_{FF}(\omega)][H(\omega)]^H \quad \textbf{(14)}$$

If the all forcing vectors are then assumed to be broadband, smooth (i.e. constant with no poles or zeros), and are applied to all degrees-of-freedoms of the system, the input cross-spectral matrix $[G_{FF}(\omega)]$ will become a constant multiple of the identity matrix.

$$[G_{XX}(\omega)] \approx C[H(\omega)][I][H(\omega)]^H \quad \textbf{(15)}$$

This shows that the output cross-spectral matrix approximates the product of the FRF matrix and the hermitian of the FRF matrix.

$$[G_{XX}(\omega)] \approx [H(\omega)][H(\omega)]^H \quad \textbf{(16)}$$

Equation 16 illustrates that the G_{XX} matrix will include the poles from both the positive and negative frequencies due to addition of the Hermitian term. The consequence of this is most apparent when examining the cross-correlation function obtained by the Inverse Fast-Fourier Transform (IFFT) of G_{XX}. Figure 1 shows both a single cross-spectrum from a G_{XX} matrix as well as the cross-correlation function of the same measurement. The function includes the converging damped exponential in the first half of the time block and a diverging damped exponential in the second half of the time block.

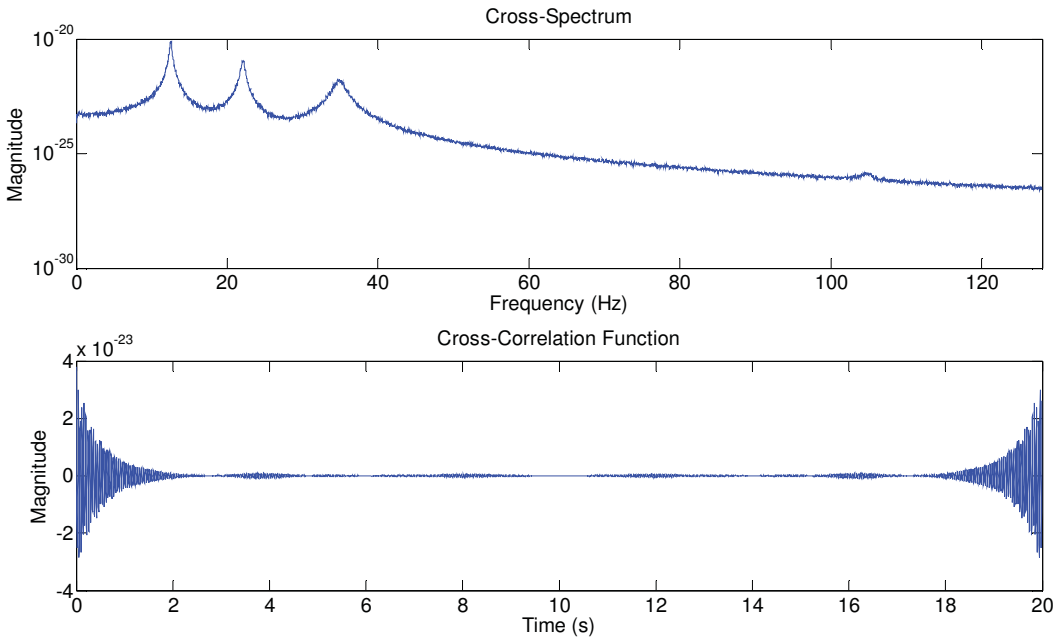

Figure 1: Cross Spectra and Cross-Correlation Function

2.1 Background Summary

All techniques used to extract modal parameters from FRF's can theoretically be used with output-only data, as the cross-spectral matrix is proportional to the FRF matrix multiplied by its Hermitian as show in Equation 16. The form shown in Equation 16 shows that the underlying system characteristics (modal parameters) are present in the G_{XX} matrix and are undistorted if all forcing function assumptions are met and all modes of the system are excited. The literature shows that studies have been conducted to show the effects of harmonic content and incomplete spatial excitation on the modal parameter estimates [15, 16, 18, 24]. It is important to note that due to the unknown constant [C] shown in Equation 15 correct scaling estimates are not available directly from OMA.

3 Modal Parameter Estimation

3.1 Damping Estimate Accuracy Concerns

It is well documented in the literature that the natural frequency estimates and modal vectors obtained from parameter estimation algorithms when using output only data are accurate. However, the damping estimates are often inaccurate [12, 13, 17]. This has been demonstrated both on theoretical cases and test cases where the use of traditional EMA techniques provides the baseline damping estimate.

A number of techniques have been investigated as methods to improve the damping estimated. These include different parameter estimation algorithms including extensions of traditional temporal modal analysis techniques as well as spatial techniques [3, 4, 5, 8, 16]. These improvements also include the use of signal processing techniques such as cyclic averaging [19, 20] to reduce leakage errors, various methods of creating spectra and the use of the Random Decrement technique [11]. However, these studies continue to show that the damping estimates are often inaccurate and accuracy can fluctuate drastically from case to case, or based upon small signal processing changes.

This paper focuses on a number of studies that were conducted to assure that the assumptions used in Equations 13 and 14 are valid.

3.2 Investigation of 5-DOF System

3.2.1 Traditional EMA Algorithms Using Output Only Data

A study was performed using the theoretical 5-DOF lumped mass system shown in Figure 2.

```
M =
   250     0     0     0     0
     0   350     0     0     0
     0     0    30     0     0
     0     0     0   450     0
     0     0     0     0    50
>> C
C =
        3250        -250           0           0           0
        -250         450        -200           0           0
           0        -200         320        -120           0
           0           0        -120         190         -70
           0           0           0         -70         270
>> K
K =
     9000000    -5000000           0           0           0
    -5000000    11000000    -6000000           0           0
           0    -6000000    12500000    -6500000           0
           0           0    -6500000    14500000    -8000000
           0           0           0    -8000000    15000000
```

Figure 2: 5-DOF Lumped Mass Model

The modal parameters of the system were determined and are shown in Table 1. The matrices were also used to create the complete FRF matrix of this system for the frequency range of 0-128Hz. This frequency range contains all modes of the system. This assures that there are no out-of-band modes affecting the parameter estimation process.

Table 1: 5-DOF System Natural Frequencies and Damping

Frequency (Hz)	Damping (% Critical)
12.526	1.149
22.083	1.059
34.864	2.172
88.524	0.487
104.779	0.847

The theoretical FRF matrix was used to calculate a cross-spectral matrix (G_{XX}) using Equation 16. This matrix will be labeled as "Theoretical G_{XX}" for all further presented test cases and is an approximation of the actual theoretical G_{XX} matrix. Forcing vectors of zero-mean random noise were applied at all degrees-of-freedom as in the form of Equation 5, using the theoretical FRF matrix to yield response time histories. These forcing functions conform to all assumptions discussed in Section 2. The response time histories of the system were then used to calculate the complete cross-spectral matrix. Care was taken when calculating the G_{XX} matrix from time histories to reduce leakage and random noise by employing windowing, cyclic averaging, and RMS averaging [14, 19, 23] as these methods have been shown to have an effect on the damping estimates [12]. The modal parameters for each data set were determined using a number of traditional modal analysis algorithms. A small amount of zero-mean random noise was added to the theoretical FRFs and cross-spectra to allow the use of these algorithms at increased model orders. Care was taken to use the same frequency resolution for all datasets, and the same parameters in the estimation algorithms. These details can be seen in Table 2. When using the time domain algorithms only the first half of the IRF was used to assure that only data from the positive frequency poles would be included in the calculation.

Table 2: Modal Parameter Estimation Algorithm Details (* If Applicable)

Algorithm Parameters	
Δf (Hz)	0.25
Frequency Band (Hz)	6.5 - 121.25
Time Band* (s)	0.5 - 1.9
Short Basis Model Order*	2 -40
Long Basis Model Order*	4 - 8

The Rational Fraction Polynomial (RFP) [21] technique was evaluated due to the frequency domain nature of the algorithm, as well as the short basis, high-order model that is well suited to

smaller datasets. The frequency domain algorithm allowed for direct use of the FRF's themselves with no data manipulations (normalization, state-space expansions, etc). Table 3 shows the natural frequencies determined for each data set. The top five rows of the table show the natural frequency values returned from RFP for the theoretical FRFs, the theoretical G_{XX} matrix calculated from Equation 16 and the calculated G_{XX}. The bottom of the table compares columns 3-5 to the theoretical values in column 2 to illustrate the error involved with each method. The frequencies are all within 1% of the theoretical values. The mode shapes were evaluated by averaging the Modal Assurance Criterion (MAC) [9] values for all modes using the modal vectors obtained from the theoretical FRFs as the reference set and the modal vectors obtained from G_{XX} as the comparison group per equation 17.

$$\frac{\sum_{r=1}^{n} MAC(r)}{n} \tag{17}$$

.Table 4 shows the damping estimates for each data set in the same format as Table 3. The estimates for the FRF and theoretical G_{XX} datasets match the theoretical values very well. However, the calculated G_{XX} dataset has considerable degradation of the estimates, especially in modes 2 and 3. The MAC values for all modes when comparing the theoretical FRFs to the theoretical and calculated G_{XX} are 1.00 showing that the modal vectors are well estimated for both cases. All error values crossing a 1% threshold are highlighted.

Table 3: Frequency Comparison Using RFP

Frequency Comparison - RFP				
Mode	**Theoretical (Hz)**	**Theoretical FRF (Hz)**	**Theoretical Gxx (Hz)**	**Calculated Gxx (Hz)**
1	12.526	12.502	12.502	12.554
2	22.083	22.040	22.040	22.099
3	34.864	34.796	34.796	34.799
4	88.524	88.352	88.350	88.613
5	104.779	104.574	104.574	104.769
% Error	N/A	0.19%	0.19%	-0.22%
% Error	N/A	0.19%	0.19%	-0.07%
% Error	N/A	0.19%	0.19%	0.19%
% Error	N/A	0.19%	0.20%	-0.10%
% Error	N/A	0.20%	0.20%	0.01%
MAC		N/A	1.00	1.00

Table 4: Damping Comparison Using RFP

Damping Comparison - RFP (All Values % Critical Damping)				
Mode	**Theoretical**	**Theoretical FRF**	**Theoretical Gxx**	**Calculated Gxx**
1	1.149	1.149	1.149	0.978
2	1.059	1.059	1.059	0.007
3	2.172	2.172	2.172	0.006
4	0.487	0.487	0.487	0.459
5	0.847	0.842	0.839	0.798
% Error	N/A	-0.03%	-0.03%	**14.85%**
% Error	N/A	-0.01%	-0.01%	**99.34%**
% Error	N/A	0.00%	0.00%	**99.72%**
% Error	N/A	0.04%	0.04%	**5.79%**
% Error	N/A	0.63%	0.98%	**5.82%**

The second-order frequency domain subspace method, Poly-Reference Frequency Domain (PFD), was evaluated [1, 6, 10]. However, due to the dataset size no valid modal parameter estimates were calculated for the G_{XX} dataset. The UMPA formulation of PFD was expanded to include model orders from 4 to 8 and evaluated. Table 5 shows that the modified PFD method yields good estimates of the natural frequencies and mode shapes for all datasets. Table 6 also again shows that the damping estimates for the calculated spectra do not correlate well with the theoretical values. The MAC values for all modes when comparing the theoretical FRFs to the

theoretical and calculated G_{XX} are 1.00 showing that the modal vectors are well estimated for both cases.

Table 5: Frequency Comparison Using Modified PFD

Frequency Comparison - Modified PFD				
Mode	**Theoretical (Hz)**	**Theoretical FRF (Hz)**	**Theoretical Gxx (Hz)**	**Calculated Gxx (Hz)**
1	12.526	12.502	12.502	12.497
2	22.083	22.040	22.040	22.097
3	34.864	34.796	34.796	34.904
4	88.524	88.350	88.350	88.547
5	104.779	104.574	104.574	104.708
% Error	N/A	0.19%	0.19%	0.23%
% Error	N/A	0.19%	0.19%	-0.06%
% Error	N/A	0.19%	0.19%	-0.12%
% Error	N/A	0.20%	0.20%	-0.03%
% Error	N/A	0.20%	0.20%	0.07%
MAC		N/A	1.00	1.00

Table 6: Damping Comparison Using Modified PFD

Damping Comparison - Modified PFD (All Values % Critical Damping)				
Mode	**Theoretical**	**Theoretical FRF**	**Theoretical Gxx**	**Calculated Gxx**
1	1.149	1.149	1.149	0.003
2	1.059	1.059	1.059	0.000
3	2.172	2.172	2.172	0.245
4	0.487	0.487	0.487	0.449
5	0.847	0.842	0.842	0.792
% Error	N/A	-0.03%	-0.03%	**99.74%**
% Error	N/A	-0.01%	-0.01%	**100.00%**
% Error	N/A	0.00%	0.00%	**88.72%**
% Error	N/A	0.04%	0.04%	**7.84%**
% Error	N/A	0.63%	0.63%	**6.53%**

The Poly-Reference Time Domain (PTD) [22] method was evaluated to determine if the use of IRF's calculated from the theoretical FRF matrix and cross-correlation functions calculated from the G_{XX} matrix had any effect on results. Table 7 shows that the natural frequencies and mode shapes are well estimated for all datasets. However, Table 8 illustrates that the damping estimate for the first mode is inaccurate when using the theoretical G_{XX} matrix and all modes are

inaccurate when using the calculated G_{XX} matrix. The modal vectors also show that they are again well estimated.

Table 7: Frequency Comparison Using PTD

Frequency Comparison - PTD				
Mode	**Theoretical (Hz)**	**Theoretical FRF (Hz)**	**Theoretical Gxx (Hz)**	**Calculated Gxx (Hz)**
1	12.526	12.488	12.486	12.482
2	22.083	22.006	22.005	22.062
3	34.864	34.734	34.734	34.801
4	88.524	88.173	88.173	88.355
5	104.779	104.361	104.361	104.503
% Error	N/A	0.31%	0.32%	0.35%
% Error	N/A	0.35%	0.35%	0.10%
% Error	N/A	0.37%	0.37%	0.18%
% Error	N/A	0.40%	0.40%	0.19%
% Error	N/A	0.40%	0.40%	0.26%
MAC		N/A	1.00	1.00

Table 8: Damping Comparison Using PTD

Damping Comparison - PTD (All Values % Critical Damping)				
Mode	**Theoretical**	**Theoretical FRF**	**Theoretical Gxx**	**Calculated Gxx**
1	1.149	1.149	1.208	0.909
2	1.059	1.059	1.059	1.084
3	2.172	2.171	2.172	2.215
4	0.487	0.487	0.487	0.494
5	0.847	0.842	0.842	0.795
% Error	N/A	-0.03%	**-5.17%**	**20.86%**
% Error	N/A	-0.01%	-0.01%	**-2.37%**
% Error	N/A	0.05%	0.00%	**-1.98%**
% Error	N/A	0.04%	0.04%	**-1.40%**
% Error	N/A	0.63%	0.63%	**6.17%**

The Eigensystem Realization Algorithm (ERA) [7] method was evaluated to determine if the use of time domain data and additional data manipulation due to the subspace nature of the technique affected the modal parameter estimates. The ERA algorithm was modified to include model orders 4 through 8 to yield more optimum results with the dataset size used. Table 9 shows that the natural frequency estimates are accurate, but the MAC calculation shows that one mode

shape is not accurate. Mode 3 was not well estimated as shown in Figure 3, although the natural frequency and damping associated with the modal vector are accurate. The damping results are similar to those obtained from PTD, where the first mode is inaccurate using the theoretical G_{XX} matrix and all modes have decreased accuracy when using the calculated G_{XX}.

Table 9: Frequency Comparison Using Modified ERA

Frequency Comparison - Modified ERA				
Mode	**Theoretical (Hz)**	**Theoretical FRF (Hz)**	**Theoretical Gxx (Hz)**	**Calculated Gxx (Hz)**
1	12.526	12.491	12.483	12.484
2	22.083	22.006	22.002	22.072
3	34.864	34.732	34.736	34.775
4	88.524	88.173	88.172	88.309
5	104.779	104.361	104.361	104.533
% Error	N/A	0.28%	0.35%	0.34%
% Error	N/A	0.35%	0.37%	0.05%
% Error	N/A	0.38%	0.37%	0.25%
% Error	N/A	0.40%	0.40%	0.24%
% Error	N/A	0.40%	0.40%	0.23%
MAC		N/A	1.00	0.82

Table 10: Damping Comparison Using Modified ERA

Damping Comparison - Modified ERA (All Values % Critical Damping)				
Mode	**Theoretical**	**Theoretical FRF**	**Theoretical Gxx**	**Calculated Gxx**
1	1.149	1.152	0.974	0.903
2	1.059	1.060	1.037	1.097
3	2.172	2.169	2.172	2.159
4	0.487	0.487	0.487	0.461
5	0.847	0.842	0.843	0.809
% Error	N/A	-0.30%	**15.20%**	**21.38%**
% Error	N/A	-0.10%	**2.07%**	**-3.60%**
% Error	N/A	0.14%	0.00%	0.60%
% Error	N/A	0.04%	0.04%	**5.38%**
% Error	N/A	0.63%	0.51%	**4.52%**

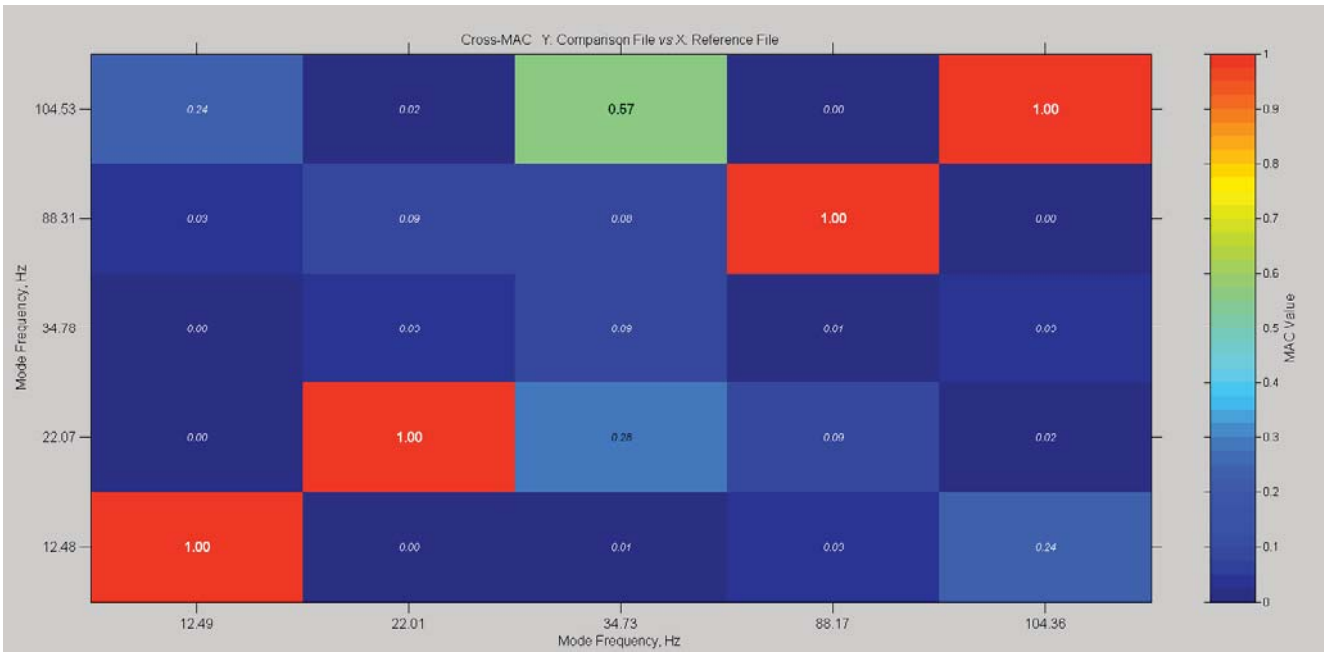

Figure 3: MAC Using Theoretical FRF's and Modified ERA

3.2.2 Effect of System Characteristics on Damping Estimates

The damping matrix for the 5-DOF system was modified and used to create two new systems one which was more heavily damped and one more lightly damped than the original system. The resulting theoretical modal parameters for the new systems are shown in Table 11. The system was again used to create a theoretical FRF matrix and subsequently a theoretical G_{XX} matrix through use of Equation 16. Response time histories due to zero-mean random noise applied at all degrees of freedom were again used to calculate a G_{XX} matrix.

Table 11: Modified 5-DOF Systems

Heavily Damped System	
Frequency (Hz)	**Damping (% Critical)**
12.526	5.743
22.083	5.295
34.864	10.860
88.524	2.436
104.779	4.237
Lightly Damped System	
Frequency (Hz)	**Damping (% Critical)**
12.526	0.230
22.083	0.212
34.864	0.434
88.524	0.097
104.779	0.169

The theoretical G_{XX} matrix and calculated G_{XX} matrix for both cases were evaluated using the PTD and RFP algorithms. The frequency comparisons and FRFs for this dataset were not included in the tables in this section. The damping estimates for the heavily damped system are shown in Table 12 (all values in % Critical). The damping estimates when using the theoretical G_{XX} matrix are similar to those of the baseline 5-DOF system, except the PTD algorithm estimated a slightly inaccurate value for the 1st system mode.

Table 12: Damping Results for Heavily Damped System

Poly-Reference Time Domain					
Mode	**True Damping**	**Gxx (Theoretical)**	**% Error**	**Gxx (Calculated)**	**% Error**
1	5.743	5.683	**1.04%**	5.6376	**1.84%**
2	5.295	5.3411	-0.88%	5.2313	**1.19%**
3	10.860	10.9368	-0.71%	9.7654	**10.08%**
4	2.436	2.4354	0.02%	2.365	**2.91%**
5	4.237	4.2082	0.67%	3.1352	**26.00%**
Rational Fraction Polynomial					
Mode	**True Damping**	**Gxx (Theoretical)**	**% Error**	**Gxx (Calculated)**	**% Error**
1	5.743	5.6932	0.87%	5.7553	-0.21%
2	5.295	5.3461	-0.97%	5.1899	**1.98%**
3	10.860	10.9404	-0.74%	7.307	**32.72%**
4	2.436	2.4357	0.01%	2.4142	0.89%
5	4.237	4.2116	0.59%	4.1429	**2.21%**

The damping estimates for the lightly damped system are shown in Table 13. The damping estimates when using the theoretical G_{XX} matrix are similar to those of the baseline 5-DOF system, although the results of using PTD are slightly more inaccurate. Both the PTD and RFP method were unable to accurately estimate the damping when using the calculated G_{XX} matrix and are more inaccurate than the heavily damped case.

Table 13: Damping Results for Lightly Damped System

Poly-Reference Time Domain					
Mode	**True Damping**	**Gxx (Theoretical)**	**% Error**	**Gxx (Calculated)**	**% Error**
1	0.230	0.1231	**46.41%**	0.1481	**35.53%**
2	0.212	0.2223	**-4.97%**	0.3038	**-43.45%**
3	0.434	0.4316	0.64%	0.4534	**-4.37%**
4	0.097	0.0975	-0.06%	0.087	**10.71%**
5	0.169	0.1724	**-1.73%**	0.1991	**-17.49%**
Rational Fraction Polynomial					
Mode	**True Damping**	**Gxx (Theoretical)**	**% Error**	**Gxx (Calculated)**	**% Error**
1	0.230	0.2298	-0.03%	0.1383	**39.80%**
2	0.212	0.2117	0.04%	0.0037	**98.25%**
3	0.434	0.4343	0.02%	0.0037	**99.15%**
4	0.097	0.0967	0.76%	0.104	**-6.73%**
5	0.169	0.1677	**1.04%**	0.1814	**-7.05%**

3.2.3 Positive/Negative Frequency Interaction

A possible contributor to the inaccuracy of damping estimates when using output-only data may be a combination of the double-sided nature of the G_{XX} matrix. This is due to the positive frequency portion of the G_{XX} matrix being contaminated by the negative poles, creating a "leakage" type effect that distorts the data. This is illustrated most clearly by Figure 4, where it

can be seen that the cross correlation function does not decay to zero when the positive time lags are complete (half the data block). The remaining positive frequency data distorts the negative frequency data and vice-versa. However, in Figure 5 where the system is heavily damped, the amount of distortion due to the positive and negative frequency data not decaying to zeros by the end of their respective time lags is minimized.

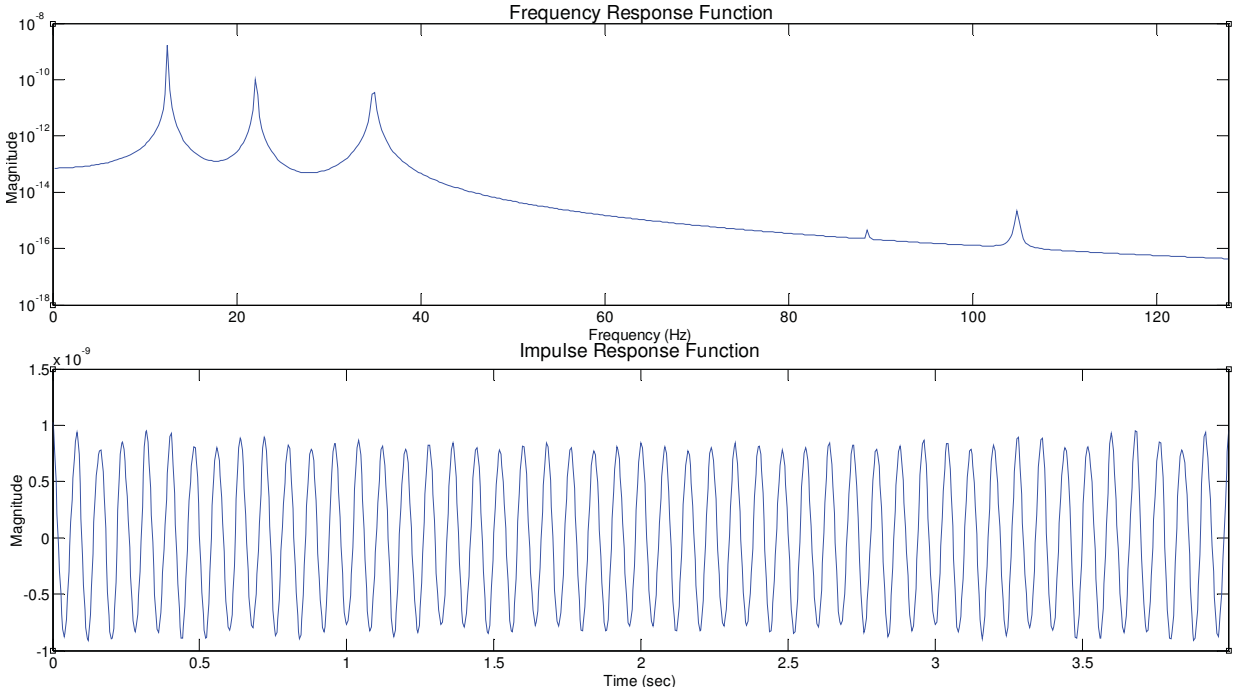

Figure 4: Lightly Damped System Cross Spectrum and Cross Correlation Function

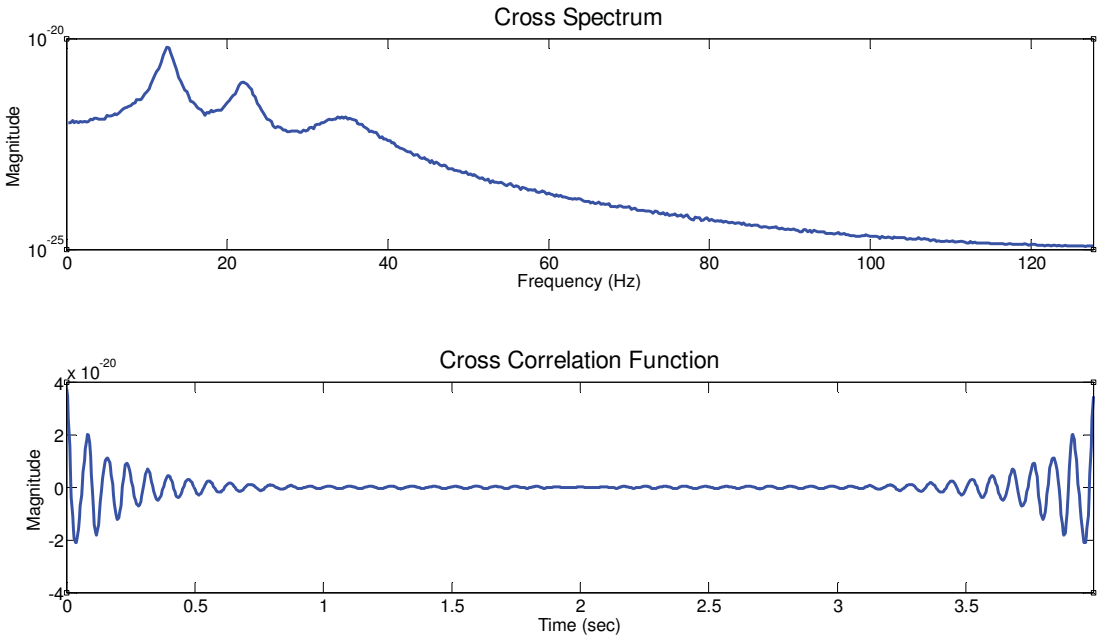

Figure 5: Heavily Damped System Cross Spectrum and Cross Correlation Function

A method employed in the literature to address the negative frequency interaction has been the Positive Power Spectra (PPS) [12]. This method uses the IFFT to transform the G_{XX} matrix to the time domain where all negative time lags are eliminated. This modified data is then transformed back to the frequency domain. Figure 6 shows a representative PPS for the heavily damped case first shown in Figure 5. This illustrates that the diverging exponential at the end of the time block has been eliminated. Care should be taken when using PPS with lightly damped systems due to truncation effects from the removal of the negative frequency data. The damping results from a PPS case are shown in Table 14, which includes the data from Table 12 for comparison. The damping results in column two are used as the baseline to compute the errors shown in columns 8 and 10. Results from PPS computed from both the theoretical G_{XX} matrix and the calculated G_{XX} are shown. It should be noted that the PPS improves the damping estimates for the calculated G_{XX}, especially when using RFP. However, it results in slightly more inaccurate results for the theoretical G_{XX} case with both PTD and RFP.

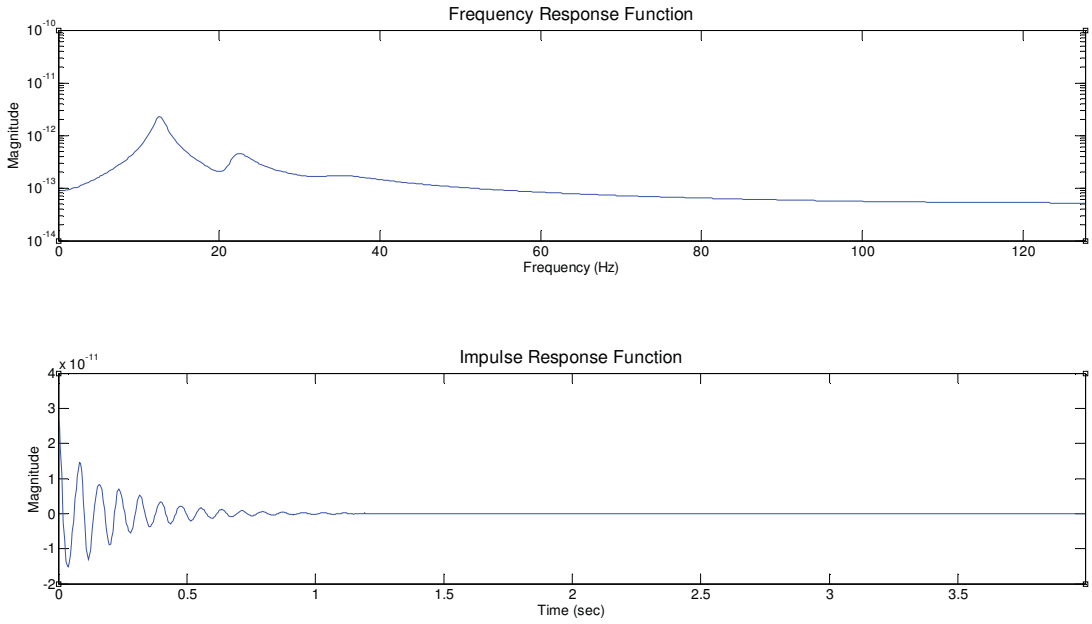

Figure 6: Heavily Damped Positive Cross Spectrum and Cross Correlation Function

Table 14: Damping Results for Heavily Damped System

Poly-Reference Time Domain									
Mode	**True Damping (% Critical)**	**Gxx (Theoretical)**	**% Error**	**Gxx (Calculated)**	**% Error**	**Gxx (Calculated PPS)**	**% Error**	**Gxx (Theoretical-PPS)**	**% Error**
1	5.743	5.683	**1.04%**	5.6376	**1.84%**	5.9097	**-2.90%**	5.667	**1.32%**
2	5.295	5.3411	-0.88%	5.2313	**1.19%**	5.3474	-1.00%	5.349	**-1.03%**
3	10.860	10.9368	-0.71%	9.7654	**10.08%**	9.6445	**11.19%**	10.933	-0.67%
4	2.436	2.4354	0.02%	2.365	**2.91%**	2.338	**4.02%**	2.415	0.86%
5	4.237	4.2082	0.67%	3.1352	**26.00%**	3.4693	**18.11%**	4.2108	0.61%
Rational Fraction Polynomial									
Mode	**True Damping (% Critical)**	**Gxx (Theoretical)**	**% Error**	**Gxx (Calculated)**	**% Error**	**Gxx (Calculated-PPS)**	**% Error**	**Gxx (Theoretical-PPS)**	**% Error**
1	5.743	5.6932	0.87%	5.7553	-0.21%	5.8884	**-2.53%**	5.5211	**3.86%**
2	5.295	5.3461	-0.97%	5.1899	**1.98%**	5.3603	**-1.24%**	5.3456	-0.97%
3	10.860	10.9404	-0.74%	7.307	**32.72%**	11.042	**-1.68%**	10.94	-0.74%
4	2.436	2.4357	0.01%	2.4142	0.89%	2.4098	**1.08%**	2.435	0.04%
5	4.237	4.2116	0.59%	4.1429	**2.21%**	4.2835	**-1.11%**	4.2046	0.75%

3.2.4 5-DOF Theoretical System Summary

When evaluating the baseline system using a full theoretical G_{xx} matrix calculated from the full FRF matrix all traditional EMA algorithms were able to correctly estimate the natural frequencies of the system with less the 1% error. However, only the frequency domain algorithms were able to estimate the damping of all modes within less than 1% error. The time domain algorithms (PTD, Modified-ERA) which operate on the IRF rather than the FRF, both were not able to determine the damping of the first system mode with less than 1% error. When using the G_{xx} matrix calculated from time histories all methods used in the study had modes with estimated damping values greater than 1% from the true values. The time domain algorithms were able to provide better estimates of the damping and only had large error (>10%) for the first system mode. The frequency domain algorithms had 3 modes with errors over 10%.

The poles surface density plots in Figure 7 through Figure 10 show a general trend when comparing the different parameter estimation methods. The frequency domain methods have very tight groups of estimated poles, indicating most model iterations return the same results. However, the time domain methods show a slight scatter of the estimated poles. This is especially true of the first mode which had greater than 1% error for both the PTD and modified-ERA methods.

It was also illustrated that the system damping itself will have an influence on the accuracy of the damping estimates due to the interaction of the positive and negative poles. The heavily damped system was shown to provide results similar to the baseline system when using the PTD and RPF algorithms. However, the lightly damped system showed inaccurate damping estimates with both algorithms.

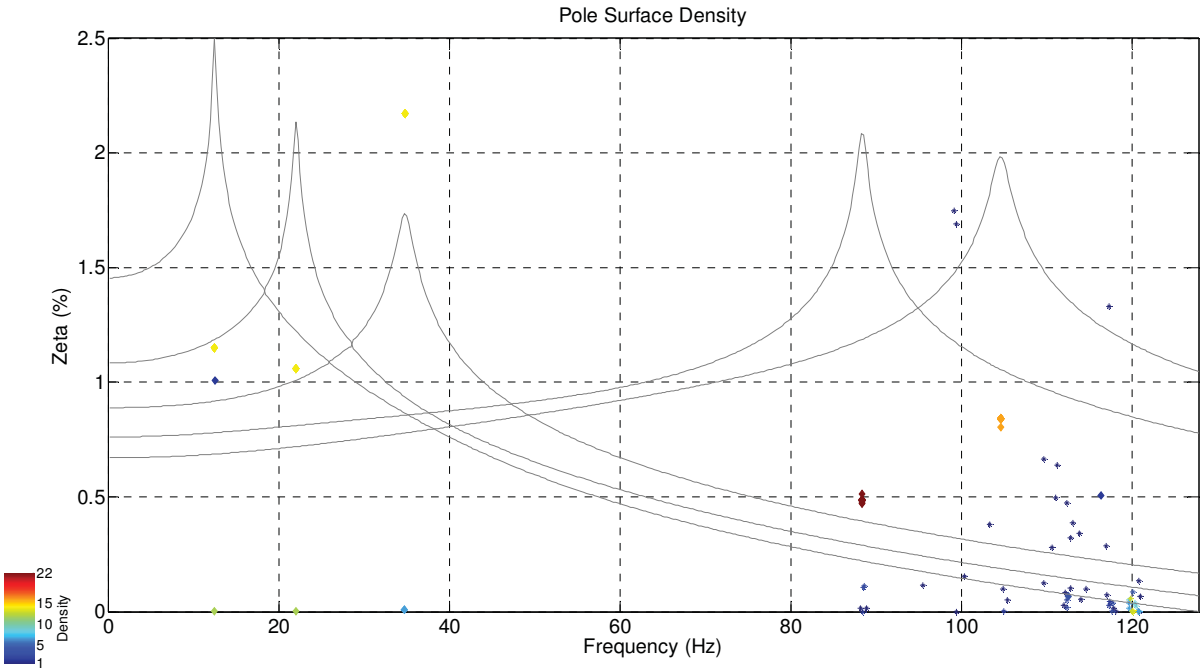

Figure 7: Pole Surface Density Utilizing RFP with Theoretical G_{xx} Data

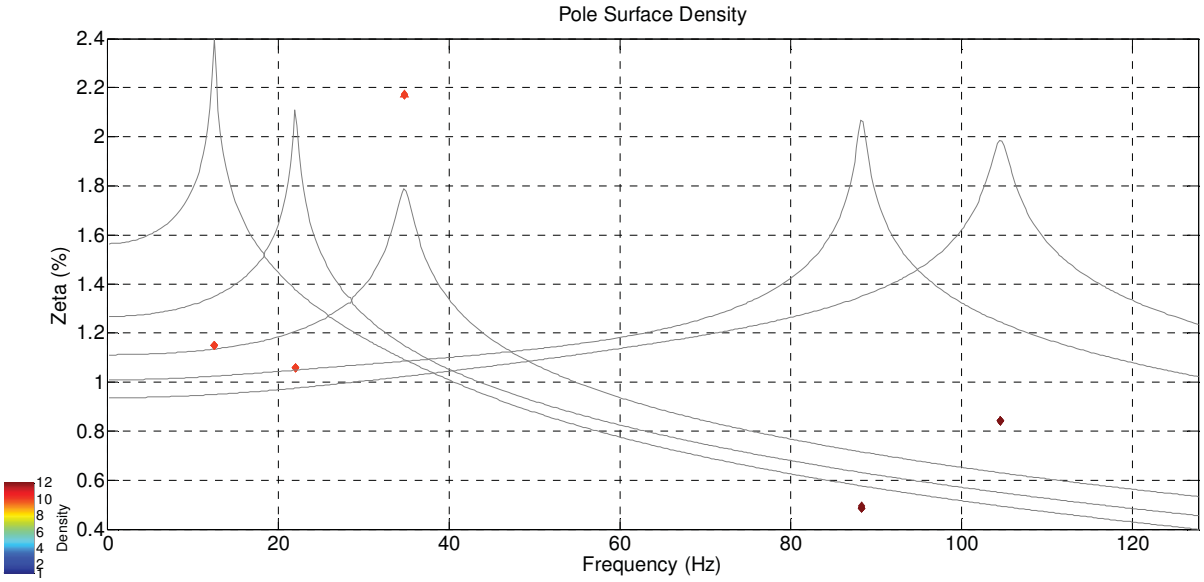

Figure 8: Pole Surface Density Utilizing Modified PFD with Theoretical G_{xx} Data

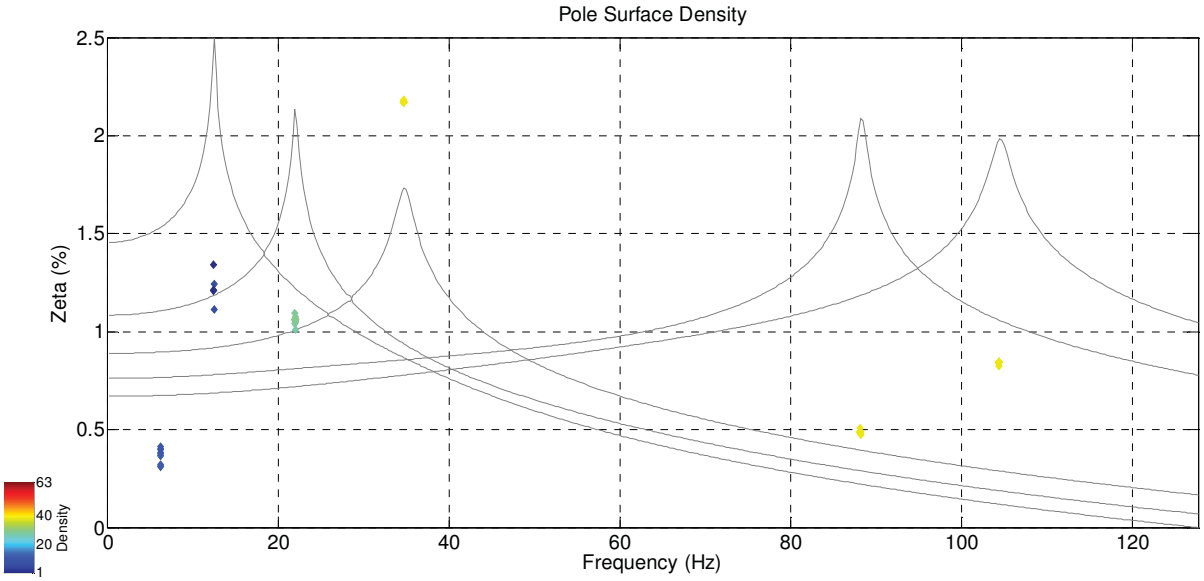

Figure 9: Pole Surface Density Utilizing PTD with Theoretical G_{xx} Data

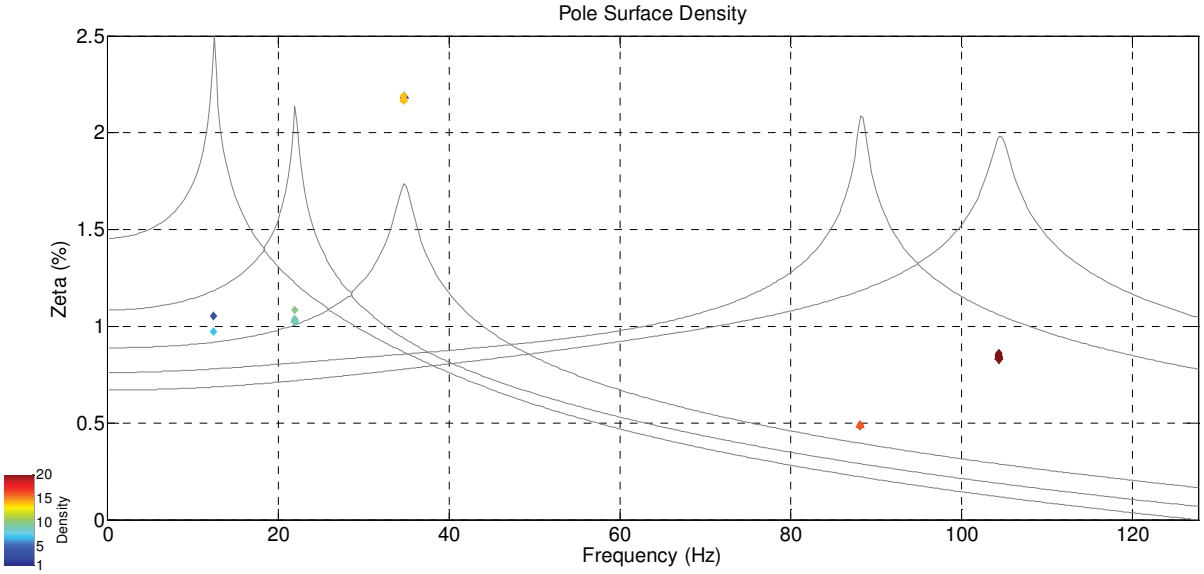

Figure 10: Surface Density Utilizing Modified ERA with Theoretical G_{xx} Data

3.2.5 Rank Deficient Systems

The 5-DOF system theoretical FRF matrix was used to create a number of rank deficient G_{XX} matrices to determine the effect on the estimated frequencies and damping. This was accomplished by removing columns from the FRF matrix and rows from the conjugate FRF matrix as shown in Equations 18 and 19.

$$G_{XX} = [H_{i,j}][H_{i,j}]^H \quad \textbf{(18)}$$

$$[G_{XX}]_{5\times5} = [H_{5\times j}][H_{i\times5}]^H \quad \textbf{(19)}$$

i = 1-5, j = 1-5

This allowed the outer product of the multiplication to yield a 5x5 G_{XX} matrix that was deficient of information. This data was then evaluated using the RFP and PTD algorithms. The same parameters shown in Table 2 were used for this evaluation. The system was evaluated in this manner first using only a single row and column of the FRF matrix as shown in Equation 20.

$$[G_{xx}]_{5x5} = \{H_{5x1}\}\{H_{1x5}\}^H \quad \textbf{(20)}$$

Table 15 shows the percent error for the damping and frequency estimates obtained from the PTD and RFP algorithms when using one row and one column of the FRF matrix to create the 5x5 G_{XX} matrix. It can be seen that for the two cases shown the PTD estimates are inaccurate. Table 16 shows two more row column combinations that yield inaccurate damping estimates with both the PTD and RFP algorithms. Additional data is included in the Appendix for reference.

Table 15: Damping Estimate Error When Using Only One Row and Column of the FRF Matrix – Examples 1 & 2

	PTD - Column 1, Row 1			PTD - Column 1, Row 5	
Mode	Frequency Percent Error	Damping Percent Error		Frequency Percent Error	Damping Percent Error
1	0.39%	**10.15%**		0.82%	**11.37%**
2	0.33%	0.93%		0.35%	**1.31%**
3	0.37%	0.05%		0.37%	-0.32%
4	0.41%	**-1.81%**		0.40%	0.25%
5	0.40%	0.15%		0.40%	0.63%
	RFP - Column 1, Row 1			RFP - Column 1, Row 5	
Mode	Frequency Percent Error	Damping Percent Error		Frequency Percent Error	Damping Percent Error
1	0.19%	-0.03%		0.19%	0.14%
2	0.19%	-0.01%		0.19%	0.18%
3	0.19%	0.00%		0.19%	0.00%
4	0.20%	0.04%		0.20%	0.04%
5	0.20%	0.51%		0.20%	0.63%

Table 16: Damping Estimate Error When Using Only One Row and Column of the FRF Matrix – Examples 3 & 4

	PTD - Column 3, Row 3			PTD - Column 4, Row 4	
Mode	Frequency Percent Error	Damping Percent Error		Frequency Percent Error	Damping Percent Error
1	-0.31%	**-58.63%**		0.58%	**-7.61%**
2	0.34%	-0.20%		0.37%	-0.29%
3	0.37%	0.00%		0.37%	0.14%
4	0.40%	**1.27%**		0.40%	0.04%
5	0.40%	0.86%		0.40%	0.63%
	RFP - Column 3, Row 3			RFP - Column 4, Row 4	
Mode	Frequency Percent Error	Damping Percent Error		Frequency Percent Error	Damping Percent Error
1	-0.01%	**1.45%**		0.19%	-0.03%
2	**2.11%**	**-300.23%**		0.19%	-0.01%
3	0.36%	**93.46%**		0.19%	0.09%
4	0.19%	-0.37%		0.20%	-0.16%
5	0.20%	0.63%		0.20%	**1.06%**

The case where only one row and column of the FRF matrix are used to create the G_{xx} matrix contains the least amount of information possible and it may be expected to create modal parameter estimate issues. The case where only one row and column are remove while creating the rank deficient G_{XX} matrix was evaluated to determine the sensitivity to the amount of data removed. Table 17 shows that even when removing very little data from the G_{XX} matrix both the PTD and RFP algorithm inaccurately estimated the damping.

Table 17: Damping and Frequency Estimates with Row 2 and Column 2 Removed

	PTD - Columns 1,3-5, Rows 1,3-5					
Mode	True Frequency	Estimated Frequency	Percent Error	True Damping	Estimated Damping	Percent Error
1	12.526	12.427	0.79%	1.149	1.5821	**-37.74%**
2	22.083	22.005	0.35%	1.059	1.029	**2.82%**
3	34.864	34.734	0.37%	2.172	2.171	0.05%
4	88.524	88.172	0.40%	0.487	0.486	0.25%
5	104.779	104.361	0.40%	0.847	0.842	0.63%
	RFP - Columns 1,3-5, Rows 1,3-5					
Mode	True Frequency	Estimated Frequency	Percent Error	True Damping	Estimated Damping	Percent Error
1	12.526	12.502	0.19%	1.149	1.149	-0.03%
2	22.083	22.04	0.19%	1.059	1.059	-0.01%
3	34.864	34.795	0.20%	2.172	2.171	0.05%
4	88.524	88.337	0.21%	0.487	0.498	**-2.22%**
5	104.779	104.576	0.19%	0.847	0.843	0.51%

3.2.6 Rank Deficiency Summary

Using a rank deficient G_{XX} matrix yielded inaccurate damping estimates in nearly all cases. In some cases the estimate accuracy was similar to the case using the full rank G_{XX} matrix. However, other cases showed a more significant decrease in accuracy of the damping estimates when compared to the full rank matrix. The RFP algorithm which yielded accurate estimates with a full rank G_{XX} matrix as shown in Section 3.1 was sensitive to the rank deficiency. Additional test cases using different row/column combinations are included in the Appendix for reference.

4 Investigation of 15-DOF System

4.1.1 Traditional EMA Algorithms Utilizing Output Only Data

The 15-DOF system shown in Figure 11 was used to generate a theoretical FRF matrix. This matrix was then used to create a theoretical G_{XX} matrix and response time histories with which a calculated G_{XX} matrix was created using standard signal processing techniques. The modal parameters were determined for the system using the RFP and PTD EMA algorithms with datasets utilizing the FRF matrix, a theoretical *Gxx* matrix and the calculated G_{XX} matrix.

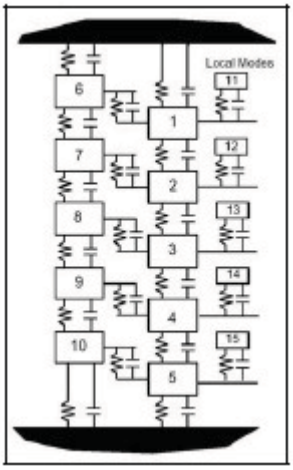

Figure 11: 15-DOF System

Table 18 shows the frequency and damping results when using the RFP algorithm. All results are compared to the true theoretical values (column 2) when computing the error. The results are similar to those of the 5-DOF system. The theoretical G_{XX} matrix yields good estimates of damping for all modes. However, when using the calculated G_{XX} matrix the damping and in some cases the frequency estimates are inaccurate. Table 19 shows similar results using the PTD algorithm. The theoretical G_{XX} inaccurately estimated the damping for mode 1, similar to that of

the 5-DOF system examined previously. It should be noted that the poor damping estimates when using the calculated G_{XX} matrix are similar to those reported in the literature [16]

Table 18: 15-DOF System Modal Parameters (Rational Fraction Polynomial)

Mode	Theoretical Frequency (Hz)	Frequency - FRF's (Hz)	% Error	Frequency - Theoretical Gxx	% Error	Frequency - Calculated Gxx	% Error
1	15.99	15.98	0.02%	15.982	0.02%	15.7434	**1.51%**
2	30.86	30.84	0.06%	30.841	0.06%	30.7631	0.31%
3	43.60	43.55	0.11%	43.551	0.11%	43.4541	0.33%
4	46.44	46.39	0.12%	46.387	0.12%	45.8287	**1.32%**
5	53.32	53.23	0.17%	53.229	0.17%	53.0225	0.55%
6	53.39	53.30	0.16%	53.303	0.16%	53.2978	0.17%
7	59.41	59.29	0.20%	59.293	0.20%	59.0974	0.53%
8	61.62	61.49	0.22%	61.488	0.22%	63.0254	**-2.27%**
9	68.81	68.62	0.27%	68.624	0.27%	67.4578	**1.97%**
10	73.63	73.40	0.31%	73.407	0.30%	72.1911	**1.95%**
11	128.84	128.69	0.11%	128.694	0.11%	128.7723	0.05%
12	136.55	136.42	0.10%	136.415	0.10%	136.3464	0.15%
13	143.86	143.73	0.09%	143.733	0.09%	143.7503	0.08%
14	150.83	150.70	0.08%	150.705	0.08%	150.742	0.06%
15	157.47	157.35	0.07%	157.353	0.07%	157.4695	0.00%
Mode	**Theoretical Damping (% Critical)**	**Damping- FRF's (% Critical)**	**% Error**	**Damping - Theoretical Gxx**	**% Error**	**Damping - Calculated Gxx**	**% Error**
1	2.01	2.01	0.02%	2.007	0.07%	1.0467	**47.88%**
2	3.87	3.87	0.01%	3.871	0.09%	3.6323	**6.25%**
3	5.47	5.47	0.01%	5.468	0.03%	5.7138	**-4.47%**
4	5.82	5.82	0.01%	5.818	0.11%	5.0517	**13.27%**
5	6.68	6.68	0.00%	6.675	0.00%	0.5867	**91.21%**
6	6.69	6.69	0.00%	6.691	0.00%	5.9067	**11.72%**
7	7.43	7.43	0.00%	7.428	0.01%	6.1397	**17.35%**
8	7.72	7.72	0.00%	7.712	0.05%	6.6823	**13.40%**
9	8.60	8.60	0.00%	8.595	0.01%	4.9953	**41.89%**
10	9.19	9.19	-0.01%	9.182	0.03%	6.3852	**30.48%**
11	5.22	5.22	-0.01%	5.218	0.01%	5.084	**2.58%**
12	4.91	4.91	-0.01%	4.91	-0.01%	4.8997	0.20%
13	4.66	4.66	0.01%	4.657	0.01%	4.5456	**2.40%**
14	4.44	4.44	0.00%	4.441	0.02%	4.0678	**8.42%**
15	4.24	4.24	0.00%	4.244	0.00%	4.2613	-0.41%

Table 19: 15-DOF System Modal Parameters (Poly-Reference Time Domain)

Mode	Theoretical Frequency (Hz)	Frequency - FRF's (Hz)	% Error	Frequency - Theoretical Gxx	% Error	Frequency - Calculated Gxx	% Error
1	15.99	15.9569	0.18%	15.9505	0.22%	16.4136	**-2.68%**
2	30.86	30.7726	0.28%	30.7726	0.28%	30.8076	0.16%
3	43.60	43.4477	0.35%	43.4477	0.35%	43.3379	0.60%
4	46.44	46.2727	0.37%	46.2743	0.37%	46.1502	0.63%
5	53.32	53.0973	0.41%	53.0973	0.41%	53.1641	0.29%
6	53.39	53.1705	0.41%	53.1689	0.42%	53.2628	0.24%
7	59.41	59.1436	0.45%	59.142	0.46%	59.029	0.65%
8	61.62	61.3319	0.47%	61.3304	0.48%	61.7728	-0.24%
9	68.81	68.4446	0.53%	68.4494	0.53%	68.9921	-0.26%
10	73.63	73.2097	0.57%	73.216	0.56%	73.4818	0.20%
11	128.84	128.3441	0.38%	128.3473	0.38%	127.507	**1.03%**
12	136.55	136.0409	0.37%	136.0393	0.37%	136.0504	0.37%
13	143.86	143.3397	0.36%	143.3381	0.36%	142.3768	**1.03%**
14	150.83	150.2916	0.36%	150.29	0.36%	149.795	0.69%
15	157.47	156.9188	0.35%	156.9236	0.35%	155.6901	**1.13%**
Mode	**Theoretical Damping (% Critical)**	**Damping- FRF's (% Critical)**	**% Error**	**Damping - Theoretical Gxx**	**% Error**	**Damping - Calculated Gxx**	**% Error**
1	2.01	1.9889	0.97%	2.0674	**-2.94%**	4.6596	**-132.01%**
2	3.87	3.8719	0.06%	3.8712	0.08%	4.5032	**-16.23%**
3	5.47	5.4671	0.04%	5.4667	0.05%	5.9863	**-9.45%**
4	5.82	5.8218	0.04%	5.8175	0.12%	5.9634	**-2.39%**
5	6.68	6.6726	0.04%	6.6723	0.04%	6.0996	**8.62%**
6	6.69	6.6882	0.04%	6.6881	0.04%	5.7652	**13.83%**
7	7.43	7.4222	0.09%	7.4267	0.03%	6.0165	**19.01%**
8	7.72	7.709	0.09%	7.7164	-0.01%	5.7786	**25.11%**
9	8.60	8.592	0.04%	8.5939	0.02%	6.3603	**26.01%**
10	9.19	9.186	-0.01%	9.1805	0.05%	5.2941	**42.36%**
11	5.22	5.213	0.11%	5.2149	0.07%	4.7999	**8.02%**
12	4.91	4.9088	0.02%	4.9047	0.10%	4.6083	**6.14%**
13	4.66	4.6567	0.02%	4.6568	0.02%	4.1899	**10.04%**
14	4.44	4.4411	0.02%	4.4427	-0.02%	2.9697	**33.14%**
15	4.24	4.2428	0.03%	4.243	0.02%	3.8708	**8.79%**

4.1.2 Rank Deficient Cases

The methods developed in 3.2.5 were extended to the 15-DOF system. The rank deficient case where 4 rows and 4 columns are used to calculate the G_{XX} matrix is shown in Table 20. The PTD and RFP algorithms were used to compare the true values for the system to those calculated from the rank deficient G_{XX} matrix. Theoretical FRF data was used as the starting point for all data presented in Section 4.1.2. The frequency estimates are shown to be accurate. However, the damping estimates using this data are only inaccurate at one mode.

Table 20: Rank Deficient 15-DOF G_{xx} Matrix (Example 1)

Mode	True Frequency (Hz)	PTD (Columns 1-4, Rows 12-15)	% Error	RFP (Columns 1-4, Rows 12-15)	% Error
1	15.985	15.9632	0.14%	15.9823	0.02%
2	30.858	30.8108	0.15%	30.841	0.06%
3	43.600	43.5018	0.23%	43.5512	0.11%
4	46.444	46.3316	0.24%	46.4255	0.04%
5	53.317	53.1657	0.28%	53.2294	0.16%
6	53.391	53.2389	0.28%	53.3026	0.17%
7	59.413	59.2184	0.33%	59.3075	0.18%
8	61.624	61.4115	0.34%	61.4863	0.22%
9	68.811	68.5385	0.40%	68.6244	0.27%
10	73.630	73.3099	0.43%	73.4039	0.31%
11	128.840	128.5208	0.25%	128.7038	0.11%
12	136.550	136.2287	0.24%	136.4149	0.10%
13	143.860	143.5355	0.23%	143.7583	0.07%
14	150.830	150.4969	0.22%	150.6927	0.09%
15	157.470	157.1575	0.20%	157.3533	0.07%
Mode	**True Damping (% Critical)**	**PTD (Columns 1-4, Rows 12-15)**	**% Error**	**RFP (Columns 1-4, Rows 12-15)**	**% Error**
1	2.008	2.0624	**-2.69%**	2.0081	0.01%
2	3.874	3.8653	0.23%	3.8746	-0.01%
3	5.469	5.468	0.03%	5.4683	0.02%
4	5.824	5.8308	-0.11%	5.8914	**-1.15%**
5	6.675	6.6742	0.01%	6.6755	-0.01%
6	6.691	6.6891	0.03%	6.691	0.00%
7	7.429	7.4273	0.02%	7.4415	-0.17%
8	7.716	7.7142	0.02%	7.7169	-0.01%
9	8.596	8.5939	0.02%	8.5962	-0.01%
10	9.185	9.1834	0.02%	9.1852	0.00%
11	5.219	5.2167	0.04%	5.2202	-0.03%
12	4.910	4.9135	-0.08%	4.9097	0.00%
13	4.658	4.6541	0.08%	4.6537	0.08%
14	4.442	4.4463	-0.10%	4.4371	0.11%
15	4.244	4.2391	0.12%	4.244	0.00%

The rank deficient case was then extended to where only one row and one column of the FRF matrix are used to create the G_{XX} matrix. The resulting modal parameter estimates are shown in Table 21. Following the pattern shown in the 5-DOF system the results when only using 1 row and 1 column are extremely degraded.

Table 21: Rank Deficient 15-DOF G_{xx} Matrix (Example 2)

Mode	True Frequency (Hz)	PTD (Column 1, Row 15)	% Error	RFP (Column 1, Row 15)	% Error
1	15.985	15.9935	-0.05%	15.9585	0.17%
2	30.858	30.8092	0.16%	30.9493	-0.30%
3	43.600	43.5305	0.16%	43.3968	0.47%
4	46.444	46.3348	0.24%	47.3056	**-1.86%**
5	53.317	53.2103	0.20%	52.2506	**2.00%**
6	53.391	53.2166	0.33%	52.3524	**1.95%**
7	59.413	59.2407	0.29%	56.0066	**5.73%**
8	61.624	61.324	0.49%	65.2535	**-5.89%**
9	68.811	68.634	0.26%	68.1629	0.94%
10	73.630	73.2765	0.48%	No Estimate	**N/A**
11	128.840	136.9178	**-6.27%**	128.2423	0.46%
12	136.550	143.5387	**-5.12%**	143.7408	**-5.27%**
13	143.860	150.9998	**-4.96%**	No Estimate	**N/A**
14	150.830	171.3621	**-13.61%**	No Estimate	**N/A**
15	157.470	179.8451	**-14.21%**	No Estimate	**N/A**
Mode	**True Damping (% Critical)**	**PTD (Column 1, Row 15)**	**% Error**	**RFP (Column 1, Row 15)**	**% Error**
1	2.008	2.0462	**-1.88%**	0.2309	**88.50%**
2	3.874	3.8735	0.02%	0.1929	**95.02%**
3	5.469	5.4789	-0.17%	0.8452	**84.55%**
4	5.824	5.8239	0.01%	0.8432	**85.52%**
5	6.675	6.6514	0.35%	0.3748	**94.39%**
6	6.691	6.6961	-0.08%	0.5207	**92.22%**
7	7.429	7.4722	-0.58%	0.4569	**93.85%**
8	7.716	7.7594	-0.56%	0.5321	**93.10%**
9	8.596	8.6315	-0.42%	0.7709	**91.03%**
10	9.185	9.1781	0.08%	No Estimate	**N/A**
11	5.219	5.1127	**2.03%**	0.009	**99.83%**
12	4.910	4.651	**5.27%**	4.6543	**5.20%**
13	4.658	4.2934	**7.82%**	No Estimate	**N/A**
14	4.442	1.8023	**59.43%**	No Estimate	**N/A**
15	4.244	0.586	**86.19%**	No Estimate	**N/A**

Figure 11 shows that the 15-DOF system consists of three rows of 5 masses linked by springs and dampers. The connections involving masses 11-15 are such that they create local modes that are relatively uncoupled from modes involving masses 6-10. These two groups of degrees-of-

freedom were used to create rank deficient datasets. The first is a dataset using rows and columns 11-15 in the theoretical G_{XX} calculation. The second uses rows and columns 6-10.

The results of using only rows and columns 11-15 in the G_{XX} calculation are shown in Table 22. These results illustrate that when using the frequency range involving all modes of the system, both PTD and RFP damping estimates are quite accurate. The first mode when using PTD is the only estimate that breaks the 1% error threshold.

Table 22: Damping Estimates – G_{XX} Using Columns 11-15 and Rows 11-15

Mode	True Damping (% Critical)	PTD (Columns 11-15, Rows 11-15)	% Error	RFP (Columns 11-15, Rows 11-15)	% Error
1	2.008	2.0534	**-2.24%**	2.0107	-0.11%
2	3.874	3.8727	0.04%	3.8989	-0.63%
3	5.469	5.4676	0.03%	5.4694	0.00%
4	5.824	5.8226	0.03%	5.8057	0.32%
5	6.675	6.6733	0.03%	6.6752	0.00%
6	6.691	6.689	0.03%	6.6912	-0.01%
7	7.429	7.4279	0.01%	7.4302	-0.02%
8	7.716	7.715	0.01%	7.7165	-0.01%
9	8.596	8.5937	0.02%	8.596	0.00%
10	9.185	9.1815	0.04%	9.1861	-0.01%
11	5.219	5.2178	0.02%	5.2185	0.00%
12	4.910	4.9093	0.01%	4.9096	0.00%
13	4.658	4.6565	0.02%	4.6572	0.01%
14	4.442	4.4413	0.02%	4.4418	0.00%
15	4.244	4.2436	0.01%	4.2436	0.01%

The effect of utilizing only a portion the frequency range containing modes was determined by limiting the frequency range used in the RFP algorithm. This method still has the ability to estimate out-of-band modes. Table 23 shows the effect of utilizing the frequency range of 80-180Hz which contains only the modes that relate to masses 11-15 in the 15-DOF system. For this case only the modes within the frequency band were estimated, but all were estimated accurately. Table 23 also shows the effect of utilizing data in the frequency range 6-80Hz which contains only the modes that relate to masses 1-10, of which none were included in the rank-

deficient G_{XX} calculation. Only one damping estimate crossed the 1% threshold when using only this data.

Table 23: Damping Estimates – Gxx Using Columns 11-15 and Rows 11-15 (Limited Frequency Ranges)

Mode	True Damping (% Critical)	PTD (Columns 11-15, Rows 11-15), 80-180Hz	% Error	RFP (Columns 11-15, Rows 11-15), 80-180Hz	% Error
1	2.008	No Estimate	**N/A**	2.0089	-0.02%
2	3.874	No Estimate	**N/A**	3.8741	0.01%
3	5.469	No Estimate	**N/A**	5.4642	0.10%
4	5.824	No Estimate	**N/A**	5.8191	0.09%
5	6.675	No Estimate	**N/A**	6.697	-0.33%
6	6.691	No Estimate	**N/A**	6.6697	0.32%
7	7.429	No Estimate	**N/A**	7.4354	-0.09%
8	7.716	No Estimate	**N/A**	7.7147	0.02%
9	8.596	No Estimate	**N/A**	8.6083	-0.15%
10	9.185	No Estimate	**N/A**	9.1867	-0.02%
11	5.219	5.221	-0.05%	5.2155	0.06%
12	4.910	4.8794	0.62%	4.9034	0.13%
13	4.658	4.6615	-0.08%	4.669	-0.24%
14	4.442	4.4324	0.22%	4.3347	**2.42%**
15	4.244	4.2037	0.95%	4.2432	0.02%

The results of using only rows and columns 6-10 in the G_{XX} calculation are shown in Table 24. These results show that the PTD algorithm estimated the damping inaccurately for the 1st mode. The local modes associated with masses 11-15 were either not estimated or the damping estimates were inaccurate. The RFP algorithm was able to accurately estimate the damping throughout the entire frequency range with rank-deficient data.

Table 24: Damping Estimates – Gxx Using Columns 6-10 and Rows 6-10

Mode	True Damping (% Critical)	PTD (Columns 6-10, Rows 6-10)	% Error	RFP (Columns 6-10, Rows 6-10)	% Error
1	2.008	2.1771	**-8.40%**	2.0084	0.00%
2	3.874	3.874	0.01%	3.8745	0.00%
3	5.469	5.4682	0.02%	5.4694	0.00%
4	5.824	5.8232	0.02%	5.8244	0.00%
5	6.675	6.6749	0.00%	6.6708	0.06%
6	6.691	6.6891	0.03%	6.691	0.00%
7	7.429	7.4268	0.03%	7.4289	0.00%
8	7.716	7.7165	-0.01%	7.7162	0.00%
9	8.596	8.5562	0.46%	8.5962	-0.01%
10	9.185	9.1866	-0.02%	9.1873	-0.03%
11	5.219	5.3368	**-2.26%**	5.2273	-0.17%
12	4.910	4.6811	**4.65%**	4.9097	0.00%
13	4.658	No Estimate	**N/A**	4.6574	0.00%
14	4.442	No Estimate	**N/A**	4.4416	0.01%
15	4.244	No Estimate	**N/A**	4.2341	0.23%

The RFP algorithm was again used to determine the effect utilizing only a smaller frequency range associated with a limited number of degrees-of-freedom. Table 25 shows that RFP was able to accurately estimate all modes in the frequency range when using the 6-80Hz range, which is associated with masses 1-10. However, no out-of-band estimates were found for the modes associated with masses 11-15. When utilizing the frequency range 80-180Hz which is associated with masses 11-15 the first and second modes were estimated inaccurately. However, it should be noted that these modes are out-of-band modes and the full rank G_{XX} matrix when using the identical frequency range also does not yield complete estimates for the 1st and 2nd modes.

Table 25: Damping Estimates – Gxx Using Columns 6-10 and Rows 6-10 (Limited Frequency Ranges)

Mode	True Damping (% Critical)	PTD (Columns 6-10, Rows 6-10), 6-80Hz	% Error	RFP (Columns 6-10, Rows 6-10), 6-80Hz	% Error
1	2.008	2.0091	-0.03%	2.254	**-12.23%**
2	3.874	3.8731	0.03%	3.7481	**3.26%**
3	5.469	5.4694	0.00%	5.4578	0.21%
4	5.824	5.8295	-0.09%	5.8261	-0.03%
5	6.675	6.6764	-0.02%	6.6746	0.01%
6	6.691	6.691	0.00%	6.6894	0.02%
7	7.429	7.4083	0.28%	7.4292	0.00%
8	7.716	7.7247	-0.11%	7.7157	0.00%
9	8.596	8.6033	-0.09%	8.5964	-0.01%
10	9.185	9.2581	-0.80%	9.1788	0.07%
11	5.219	No Estimate	**N/A**	5.2036	0.29%
12	4.910	No Estimate	**N/A**	4.9083	0.03%
13	4.658	No Estimate	**N/A**	4.6577	0.00%
14	4.442	No Estimate	**N/A**	4.441	0.02%
15	4.244	No Estimate	**N/A**	4.2413	0.06%

5 Calculated *Gxx* Damping Estimates

5.1.1 Non-Zero G_{FF} Off-Diagonal Terms

It has been shown that the when using the G_{XX} matrix calculated from time history data the damping estimates are often inaccurate. The G_{FF} matrix is assumed per Equation 15 to be similar to an identity matrix. However, when using uncorrelated, zero-mean random noise the G_{FF} matrix has off-diagonal terms that are nearly the same order of magnitude as the diagonal terms. Using the forcing vector created for the 5-DOF system the G_{FF} matrix is calculated. Figure 12 shows the principal components of the G_{FF} matrix illustrating that the forces are truly uncorrelated and random.

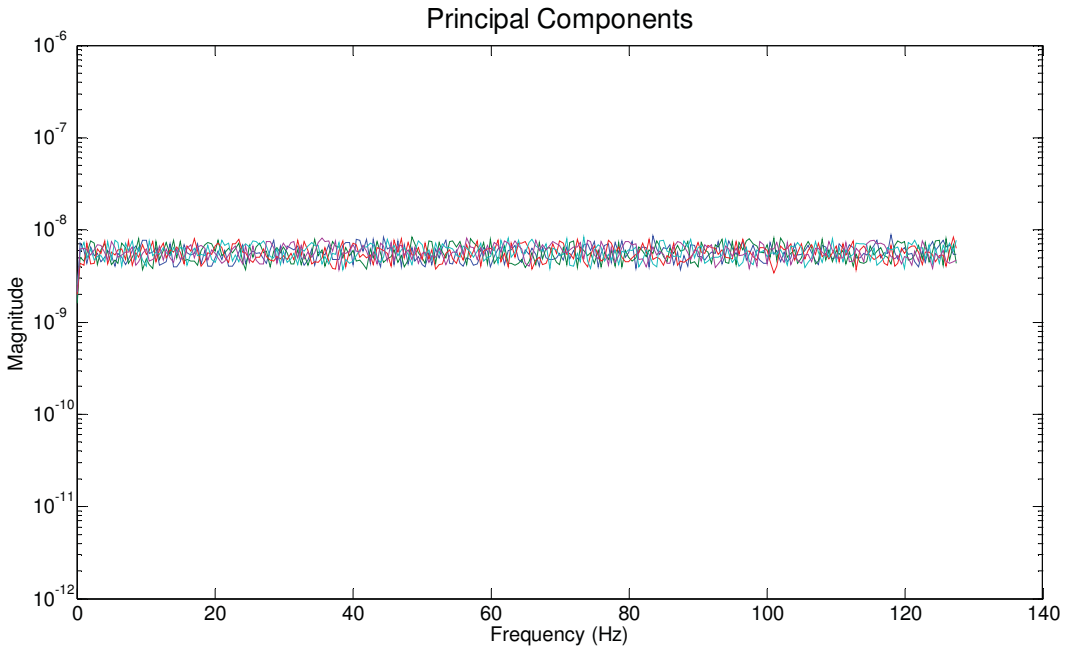

Figure 12: 5-DOF Forcing Function Principal Components

However, when examining the individual elements of any single frequency line of the G_{FF} matrix as shown in Figure 13, it becomes apparent that most of the off diagonal terms are only approximately 2 orders of magnitude smaller than the terms on the diagonal.

0.93827	0.10752 - 0.0029164i	0.030132 + 0.040374i	0.083598 - 0.041826i	-0.024286 - 0.00076839i
0.10752 + 0.0029164i	1	0.043068 + 0.00059131i	0.09835 + 0.051076i	-0.025441 + 0.077067i
0.030132 - 0.040374i	0.043068 - 0.00059131i	0.88662	-0.066696 - 0.063615i	0.0049335 - 0.015866i
0.083598 + 0.041826i	0.09835 - 0.051076i	-0.066696 + 0.063615i	0.83981	-0.020527 - 0.012983i
-0.024286 + 0.00076839i	-0.025441 - 0.077067i	0.0049335 + 0.015866i	-0.020527 + 0.012983i	0.97846

Figure 13: Elements of Frequency Line 2 of G_{FF} Matrix

5.1.2 Phase Differences

The phase information in the FRF matrix is present for all input/output combinations. However, in the theoretical G_{XX} matrix the "Driving-Point" locations (the diagonal terms) that are auto-power spectra rather than cross-power spectra lose their phase information due to the $[H][H]^{H}$ calculation. This is illustrated in Figure 14 and Figure 15 . However, it can be seen in Figure 14 that the PPS contains phase information similar to the FRF with a linear bias. The cause of this linear bias is not examined in this thesis. The calculated G_{XX} matrix is included to show that some non-zero phase information may be present. This can be reduced through the use of spectral averaging.

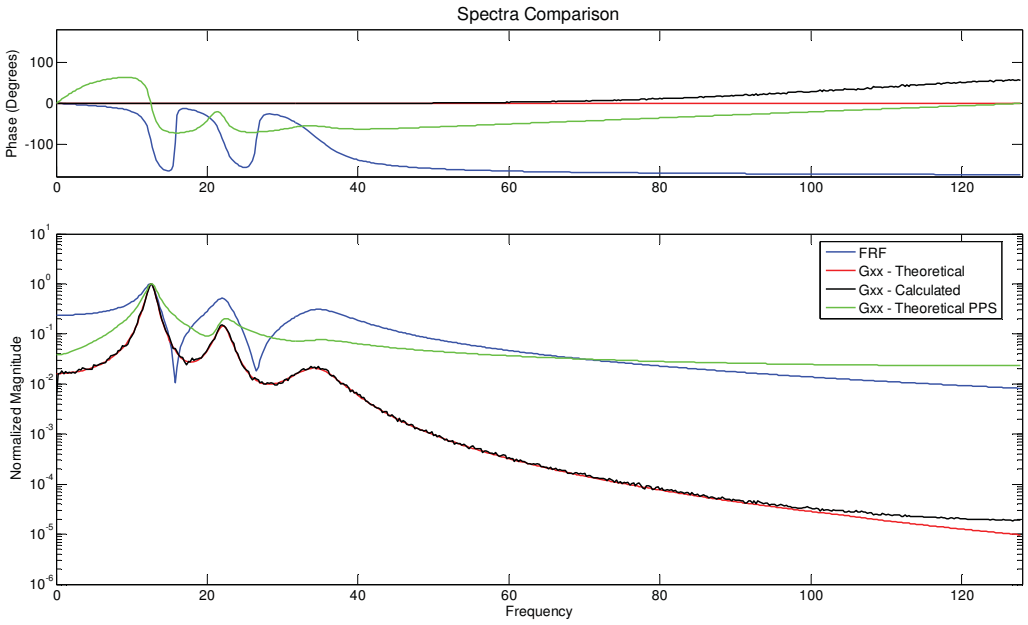

Figure 14: Magnitude and Phase Information for Driving Point Measurement (Heavily Damped System)

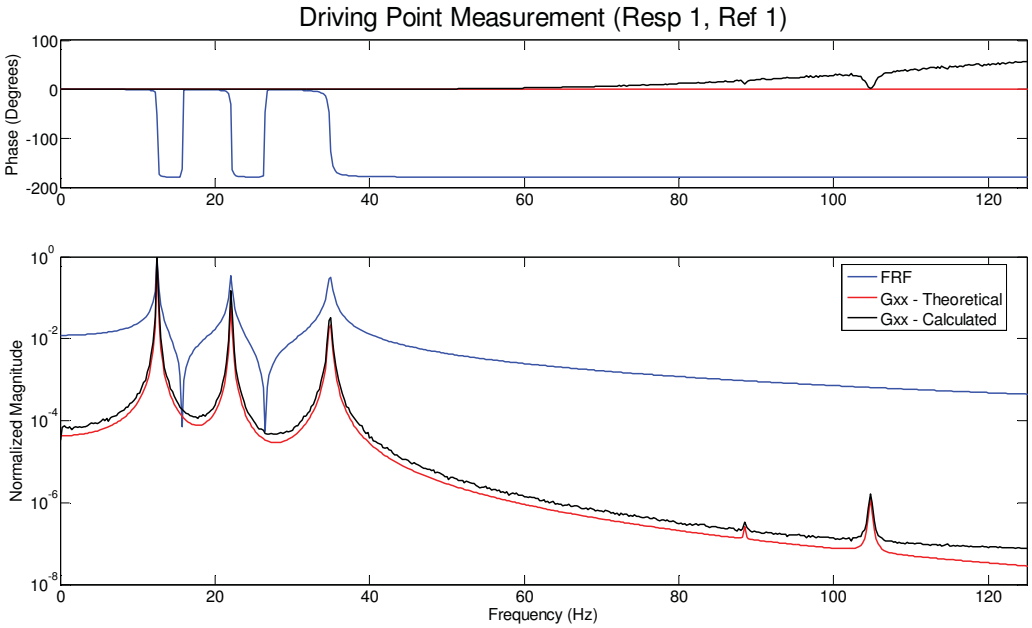

Figure 15: Magnitude and Phase Information for Driving Point Measurement

The phase information in off-diagonal or cross-spectral terms of the G_{XX} matrix is also different from the FRF. The phase angle for the cross-spectrum goes through a 180 degree shift at the anti-resonance rather than the resonance as shown near 30Hz in Figure 16. It should also be noted that if the FRF for a particular measurement contains a zero (anti-resonance) between two resonances, the corresponding cross-spectrum will contain no zero within the same frequency range. The converse is also true; where the FRF contains no anti-resonance the cross-spectra will contain an anti-resonance. This is also shown in Figure 16.

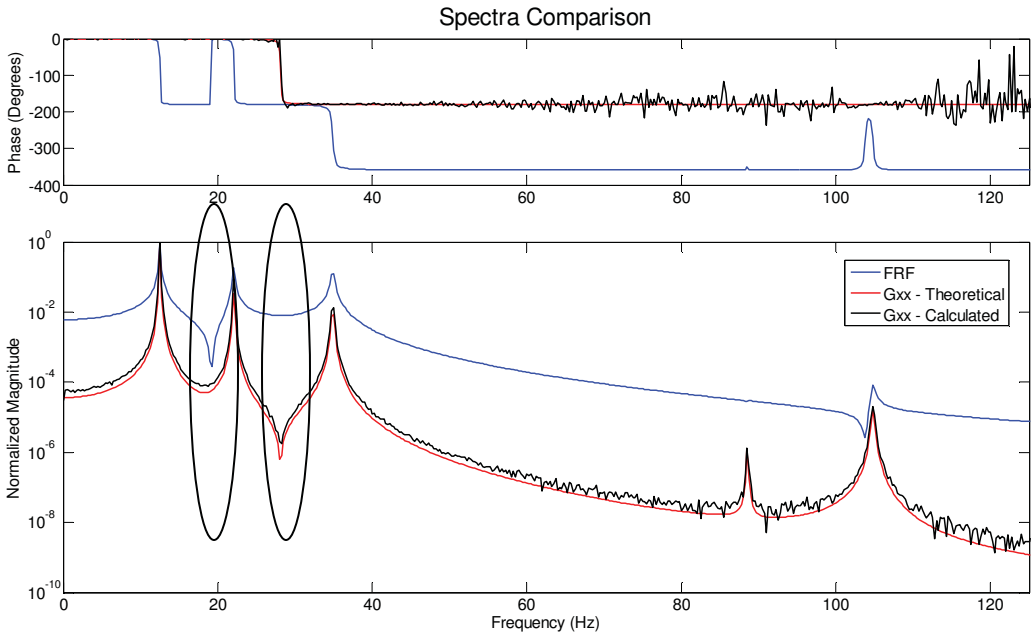

Figure 16: Magnitude and Phase Information for Off-Diagonal Measurement

When examining the phase of the entire 5-DOF as a collection of spectra an interesting pattern is revealed. Figure 17 shows that the phase shift of 180 degrees begins near the frequency of the 1st mode as would be expected.

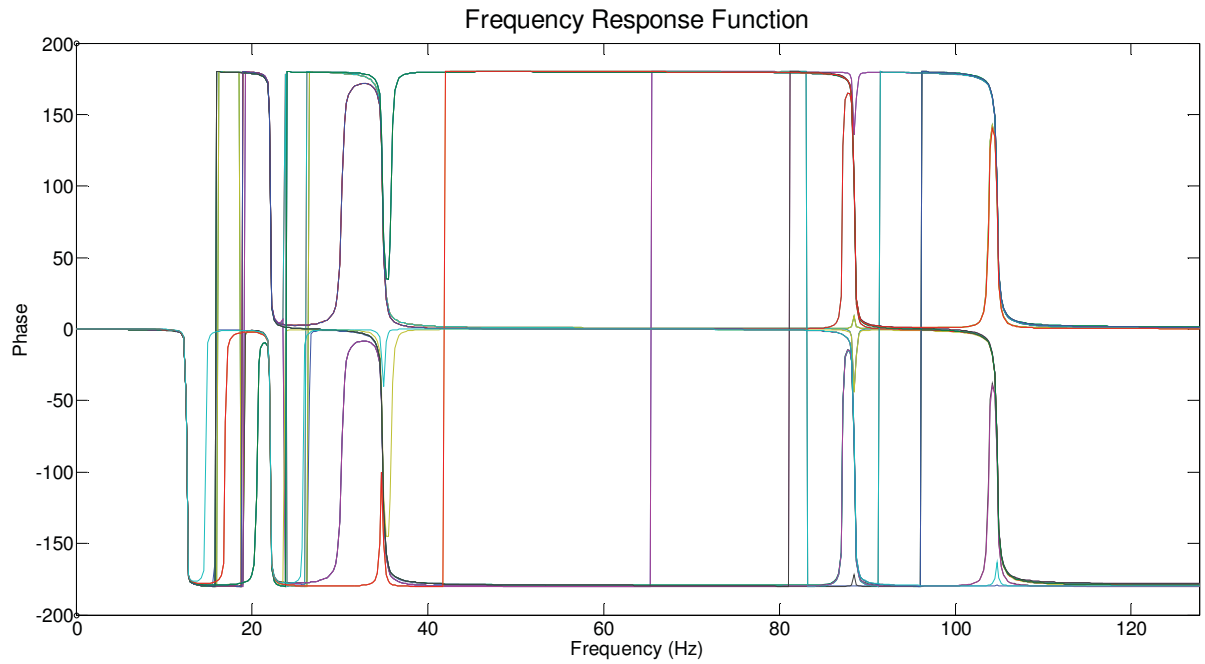

Figure 17: Phase of FRF Collection

Figure 18 shows that when using the theoretical or calculated G_{XX} matrices as a collection no single spectrum has any phase shift until after the frequency of the 1st mode in the system.

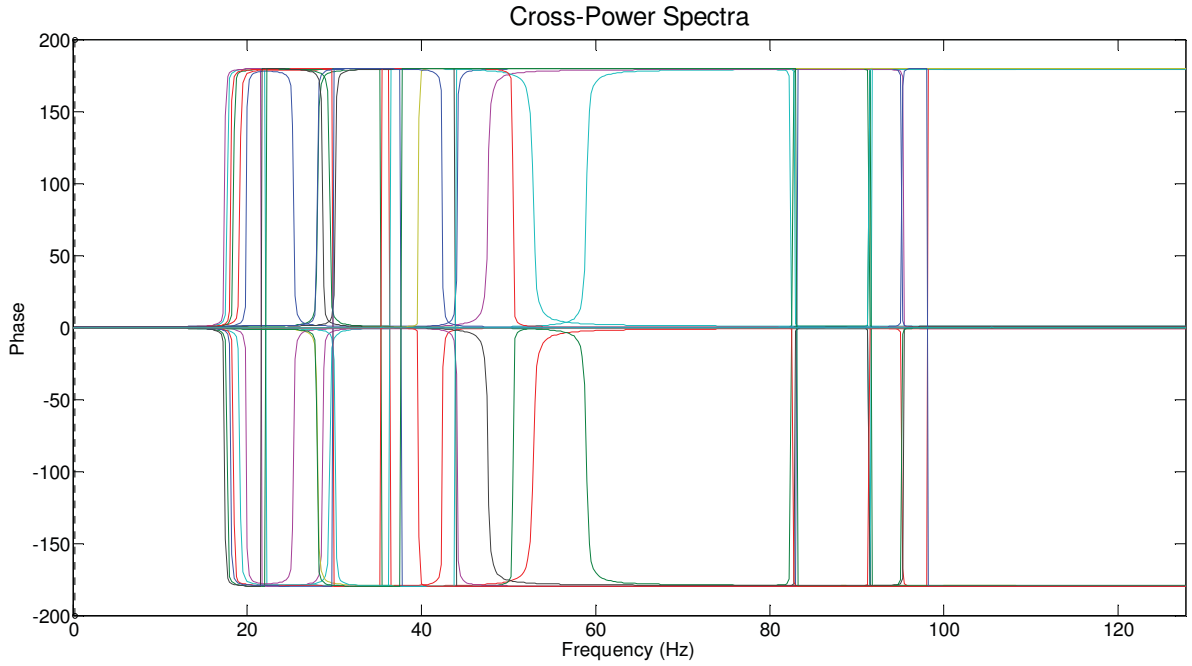

Figure 18: Phase of Theoretical Gxx Collection

6 Conclusions and Future Work

The damping estimates when using traditional EMA algorithms with output-only data were examined. 5-DOF and 15-DOF systems were used to evaluate the effects of damping and rank deficiency on the damping estimates. Interesting observations were also made concerning the phase of the cross-spectra when compared to a traditional FRF.

The use of theoretical FRF's to create an approximation of the theoretical G_{XX} matrix allows the accurate estimation of modal parameters when using frequency domain algorithms. However, the elimination of data through the use of rank deficient cases or the use of time-domain techniques affects the damping estimates. This appears to indicate that any data manipulation affects the data in a way that provides more inaccurate damping results. The calculated G_{XX} matrix consistently provides inaccurate damping results. This will be exacerbated in experimental test data by possible input coloration or correlation as well as incomplete spatial excitation. This thesis shows that inaccurate damping estimates are calculated for all modes in at least one of the test cases. These results indicate that if accurate damping estimates are required the use of traditional modal analysis or other methods may be required to achieve the desired accuracy.

Future work could involve more detailed methods to assure that there is no positive/negative frequency interaction. The investigation of the phase differences between the FRF and cross-spectra may also prove to be helpful in further determining the source of damping inaccuracy. Statistical analysis of all calculated poles from these techniques may prove useful in recognizing patterns or causes of the damping inaccuracies detailed previously. This analysis could also involve the attempt to characterize why certain modes appear to be more affected by inaccurate damping estimates than others.

7 Appendix A

Table 26: Damping Estimate Error When Using Only One Row and Column of the FRF Matrix (Examples 5 & 6)

	PTD - Column 2, Row 4			PTD - Column 3, Row 5	
Mode	Frequency Percent Error	Damping Percent Error		Frequency Percent Error	Damping Percent Error
1	0.55%	**-63.16%**		0.26%	**-4.82%**
2	0.39%	**-2.28%**		0.38%	0.65%
3	0.37%	0.18%		0.37%	0.00%
4	0.40%	0.04%		0.40%	-0.16%
5	0.40%	0.63%		0.40%	0.39%
	RFP - Column 2, Row 4			RFP - Column 3, Row 5	
Mode	Frequency Percent Error	Damping Percent Error		Frequency Percent Error	Damping Percent Error
1	0.19%	-0.47%		-0.02%	**1.79%**
2	0.19%	-0.01%		0.23%	**95.37%**
3	0.19%	-0.18%		0.38%	**95.99%**
4	0.19%	0.04%		0.20%	0.04%
5	0.20%	0.98%		0.20%	0.63%

Table 27: Damping Estimate Error When Using Only One Row and Column of the FRF Matrix (Examples 7 & 8)

	PTD - Column 1, Row 3			PTD - Column 2, Row 2	
Mode	Frequency Percent Error	Damping Percent Error		Frequency Percent Error	Damping Percent Error
1	-0.56%	**-92.06%**		0.39%	**10.15%**
2	0.34%	-0.58%		0.33%	0.93%
3	0.38%	0.05%		0.37%	0.05%
4	0.40%	0.25%		0.41%	**-1.81%**
5	0.40%	0.51%		0.40%	0.15%
	RFP - Column 1, Row 3			RFP - Column 2, Row 2	
Mode	Frequency Percent Error	Damping Percent Error		Frequency Percent Error	Damping Percent Error
1	0.19%	-0.03%		0.19%	-0.03%
2	0.19%	-0.01%		0.19%	-0.01%
3	0.19%	0.00%		0.19%	0.00%
4	0.19%	0.04%		0.20%	0.04%
5	0.20%	0.63%		0.20%	0.51%

Table 28: Damping Estimate Error – 15DOF Rank Deficient System – Limited Frequency Range

Mode	True Damping	PTD (Columns 6-10, Rows 6-10), 80-180Hz	% Error	RFP (Columns 6-10, Rows 6-10), 80-180Hz	% Error
1	2.008	No Estimate	**N/A**	2.254	**-12.23%**
2	3.874	No Estimate	**N/A**	3.7481	**3.26%**
3	5.469	No Estimate	**N/A**	5.4578	0.21%
4	5.824	No Estimate	**N/A**	5.8261	-0.03%
5	6.675	No Estimate	**N/A**	6.6746	0.01%
6	6.691	No Estimate	**N/A**	6.6894	0.02%
7	7.429	No Estimate	**N/A**	7.4292	0.00%
8	7.716	No Estimate	**N/A**	7.7157	0.00%
9	8.596	No Estimate	**N/A**	8.5964	-0.01%
10	9.185	No Estimate	**N/A**	9.1788	0.07%
11	5.219	5.2105	0.16%	5.2036	0.29%
12	4.910	4.9024	0.15%	4.9083	0.03%
13	4.658	4.6507	0.15%	4.6577	0.00%
14	4.442	4.436	0.14%	4.441	0.02%
15	4.244	4.2382	0.14%	4.2413	0.06%

Table 29: Damping Estimate Error – 15DOF Rank Deficient System – Limited Frequency Range

True Damping	PTD (Columns 11-15, Rows 11-15), 6-80Hz	% Error	RFP (Columns 11-15, Rows 11-15), 6-80Hz	% Error
2.008	2.0369	**-1.42%**	2.0091	-0.03%
3.874	3.8717	0.07%	3.8731	0.03%
5.469	5.4672	0.04%	5.4694	0.00%
5.824	5.8493	-0.43%	5.8295	-0.09%
6.675	6.6733	0.03%	6.6764	-0.02%
6.691	6.6891	0.03%	6.691	0.00%
7.429	7.4217	0.10%	7.4083	0.28%
7.716	7.7081	0.10%	7.7247	-0.11%
8.596	8.6312	-0.41%	8.6033	-0.09%
9.185	9.1025	0.90%	9.2581	-0.80%
5.219	No Estimate	**N/A**	No Estimate	**N/A**
4.910	No Estimate	**N/A**	No Estimate	**N/A**
4.658	No Estimate	**N/A**	No Estimate	**N/A**
4.442	No Estimate	**N/A**	No Estimate	**N/A**
4.244	No Estimate	**N/A**	No Estimate	**N/A**

8 References

[1] R.J. Allemang, D.L. Brown, W.A. Fladung, *Modal Parameter Estimation: A Unified Matrix Polynomial Approach*, Proceedings of the 12th International Modal Analysis Conference, 1994, pp. 501-513.

[2] J. Bendat, A. Piersol, *Random Data: Analysis and Measurement Procedures*, 2nd edition, Wiley, New York, 1986.

[3] R. Brinker, L. Zhang, P. Andersen, *Output-Only Modal Analysis by Frequency Domain Decomposition*, Proceedings of ISMA25, 2000.

[4] R. Brinker, C. Ventura, P. Andersen, *Damping Estimation by Frequency Domain Decomposition*, Proceedings of the 19th International Modal Analysis Conference, 2001

[5] S.R. Ibrahim, R. Brinker, J.C. Asmussen, *Modal Parameter Indentification From Response of General Unknown Random Inputs,* Proceedings of the 14th International Modal Analysis Conference, 1996

[6] W.A. Fladung, *A Generalized Residuals Model for the Unified Matrix Polnomial Approach to Frequency Domain Modal Parameter Estimiation*, Doctor of Philosophy Dissertation, 2001.

[7] J.N. Huang, R.S. Pappa, *An Eigensystem Realization Algorithm For Modal Parameter Identification and Model Reduction*, Journal of Guidance, Control, and Dynamics., 8(5), 1977, pp. 620-627

[8] N. Moller, R. Brinker, H. Herlufsen, P. Andersen, *Modal Testing of Mechanical Structures Subject to Operational Excitation Forces*, Proceedings of the 19th International Modal Analysis Conference, 2001

[9] R.J. Allemang, D.L. Brown, *A Correlation Coefficient for Modal Vector Analysis,* Proceedings of the International Modal Analysis Conference and Exhibition, 1982, pp. 110-116.

[10] B.Cauberghe, *Application of Frequency Domain System Identification for Experimental and Operational Modal Analysis*, PhD Dissertation, Department of Mechanical Engineering, Vrije Universiteit Brussel, Belgium, 2004.

[11] J. Rodrigues, R. Brinker, P. Andersen, *Improvement of Frequency Domain Output-Only Modal Indentification from the Application of the Random Decrement Technique*, Proceedings of the 22nd International Modal Analysis Conference, 2004

[12] S. Chauhan, *Parameter Estimation and Signal Processing Techniques for Operational Modal Analysis,* Doctoral Dissertation, University of Cincinnati, 2008

[13] P.Avitable, *Someone Told Me That Operating Modal Analysis Produces Better Results*, Modal Space – Back to Basics, 2006

[14] R.J. Allemang, D.L. Brown, *Cyclic Averaging for Frequency Response Function Estimation,* Proceedings of the 14th International Modal Analysis Conference, 1995

[15] R. Brinker, P. Andersen, N. Moller, *An Indicator for Separation of Structural and Harmonic Modes in Output-Only Modal Testing*, Proceedings of the 18th International Modal Analysis Conference, 2000

[16] S. Chauhan, R. Martell, R.J. Allemang, D.L. Brown, *Considerations in the Application of Spatial Domain Algorithms to Operational Modal Analysis*, Proceedings of ISMA International Conference on Noise and Vibrations Engineering, Katholieke Univesiteit Leuven, 2006

[17] S. Chauhan, A.W. Phillips, R.J. Allemang, *Damping Estimation Using Operational Modal Analysis*, Proceedings of the 26th International Modal Analysis Conference, 2008

[18] N.J. Jacobsen, *Separating Structural Modes and Harmonic Components in Operations Modal Analysis,* Proceedings of the 24th International Modal Analysis Conference, 2006

[19] A.W. Phillips, R.J. Allemang, A.T. Zucker, *An Overview of MIMO-FRF Excitation/Averaging Techniques*, Proceedings of the ISMA Internationsl Conference on Noise and Vibration Engineering, Katholieke Universiteite Leuven, 1998

[20] A.W. Phillips, R.J. Allemang, A.T. Zucker, *Frequency Resolution Effects on FRF Estimation: Cyclic Averaging vs. Large Block Size*, Proceedings of the 17th International Modal Analysis Conference, 1999.

[21] M. Richardson, D. Formenti, *Parameter Estimation From Frequency Response Measurements Using Rational Fraction Polynomials*, Proceedings of the 1st International Modal Analysis Conference, 1982

[22] H. Vold, T. Rocklin, J. Kundrat, R. Russell, *A Multi-Input Modal Estimation Algorithm for Mini-Computers*, SAE Transactions, Volume 91, Number 1, pp. 815-821, 1982

[23] C. Van Karsen, R.J. Allemang, *Averaging for Improved Frequency Response Functions*, Sound and Vibration, Vol 18, Number 8, pp. 18-26, 1984

[24] L. Zhang, H. Kanda, D.L. Brown, R.J. Allemang, *A Polyreference Frequency Domain Method for Modal Parameter Estimation*, ASME Paper Number 85-DET-106, 1985